NONLINEAR ANALAYSIS AND BIOMARKERS IN NEUROLOGICAL DISEASES (TEMPORAL LOBE EPILEPSY AND ALZHEIMER'S DISEASE)

by

Jinyao Zhang

A dissertation submitted in partial fulfillment
of the requirements for the degree of
Doctor of Philosophy
(Physics)
in The University of Michigan
2009

Doctoral Committee:

Professor Robert S. Savit, Chair
Professor Bradford G. Orr
Professor Leonard M. Sander
Associate Professor Michal R. Zochowski
Assistant Professor Zhaohui Qin

DEDICATION

To my parents, who always supported me unconditionally

To my wife Chun, the sweetest girl in the world

ACKNOWLEDGEMENTS

Special thanks are due to Dingzhou Li, who has provided constant help and many inspiring suggestions to this study. I also like to thank Dr. Lawrence Hudson and Dr. Daniela Minecan for their extensive collaborating in clinical reading of the EEG data, and Center for the Study of Complex Systems at the University of Michigan for providing administration and technical supports for computing resources. Finally, I would like to give my deepest gratitude to Prof. Robert Savit, who has brought me into this wonderful area and supported me all along.

TABLE OF CONTENTS

LIST OF TABLES

Tables

LIST OF FIGURES

Figures

LIST OF APPENDICES

CHAPTER 1

NONLINEAR DYANMICAL METHODS FOR SCALP ELECTROENCEPHALOGRAPHY

1.1 Introduction

1.1.1 The Mechanisms of Electroencephalography

The actions of a single neuron provide limited information of the brain cortex functions. To better understand how brain is functioning, it is helpful to observe the summated activities of neuronal ensembles. The electroencephalogram (EEG) is such a time series of wave-like voltage fluctuations that record the activities of large ensembles of neurons in the brain cortex. It is often used to show the type and location of brain activity, or to monitor and evaluate the problems associated with brain function disorders.

There are two common approaches to recording electrical responses of brain activity: intracranial EEG and scalp EEG. For intracranial EEG, electrodes are placed under the scalp and skull, either directly on the brain surface using micro-electrodes or into deep areas of the brain using very thin wires. For scalp EEG, which is less invasive, electrodes are placed on the surface of the scalp. In a typical EEG set-up, a group of active electrodes as well as one reference electrode are used to recode data. Active electrodes are set up to recode neuronal activities, while reference electrode is placed at some distance from active electrodes to recode the

baseline signal. Electrodes frequently used as the reference electrode are the ear electrodes and electrodes placed on the centerline of the brain.

EEG recordings, basically, are electrical potential differences (channels) measured between active electrodes and the reference electrode, which reflect cortical neuron activities in the area underlying the active electrodes (Kandel et al., 2000). The manner in which EEG produces each channel or trace of brain activity by using combinations of electrodes is called a montage. Besides the common reference montage, in which the ear electrodes or centerline electrodes are used, there are two other types of montage: average reference montage and bipolar montage. In average reference montage, activities from all electrodes are averaged and passed as the reference. In bipolar montage, electrodes are linked sequentially in straight lines, either from front to back (longitudinal) or left to right (traverse), such that adjacent channels always have one electrode in common. Bipolar montage is often used in clinical practice to locate the origin of local events, whereas common reference montage and average reference montage are more widely used in EEG research.

EEG data are usually analyzed in frequency and spatial domains. The typical frequency bands of rhythmic brain activities are delta (1-4Hz), theta (4-7Hz), alpha (7-13Hz), beta (13-30Hz), and gamma (30-37Hz) bands. They have different amplitudes and are associated with different behavior states. Delta waves are generally associated with sleep. They have large amplitudes compared with brain waves from other frequency domains. Theta waves occur during active behaviors and states of still alertness. Alpha waves, also called Berger rhythm, are commonly

detected during waking relaxation, opening eyes, drowsiness and sleep. Beta waves have small amplitudes and they are associated with waking consciousness. Gamma waves are associated with perception and consciousness. The spatial domain of scalp EEG usually covers the whole span of the brain, including fontal, occipital, parietal, and temporal lobes regions. Sometimes, the spatial domain is also divided differently according to the pathology of the disease. For example, focal epileptic seizures originate in a focal region and spread to other parts of the brain, thus the spatial domain may be divided into ipsilateral (the same hemisphere of seizure origination) and contralateral (the opposite hemisphere of seizure origination) regions. In our study, we investigate several statistical models that are controlled for spatial domain, and explore changes in synchronization (phase coherence) in scalp EEG recordings for temporal lobe epilepsy and Alzheimer's disease.

In general, intracranial EEG and scalp EEG recordings have their own advantages and disadvantages. For instance, intracranial EEG is not only less noisy than scalp EEG, but also sensitive to a smaller volume of neural activity. It reveals a more detailed picture of the brain near the position of the electrode. On the other hand, scalp EEG data are easy and inexpensive to obtain, and the procedures are entirely non-invasive. Moreover, scalp data, which can be recorded from any region of the brain, is particularly appropriate to the study of ictogenesis because a seizure event, even in the case of focal epilepsies, often involves parts of the brain distant from the seizure focus. In contrast, intracranial electrodes, which are implanted for clinical monitoring prior to surgery, are typically placed in limited regions of the brain,

often near, or contralateral to, a suspected region of pathological focus. Thus, scalp EEG recordings, although plagued by somewhat noise and attenuation problems, are the data of our choice to study for learning about the large scale dynamics of the epileptic brain.

1.1.2 Nonlinear Structures in Brain Electrical Activity

There are two important features in the mathematical definition of nonlinearity. First, a small change in input may produce an incommensurably large change in response. Second, the superposition principle does not hold. In this study, by "nonlinear" with reference to a time series, we mean all the information from the time series that is not included in the following sets of information:

(i) The coefficients of a linear auto regressive fit to the data.

(ii) The power spectrum.

(iii) The values of all the linear two-point correlation functions.

All other information, including information that involves the phases of the Fourier coefficients constitutes nonlinear information about a time series. Actually, the three sets of linear information given above are equivalent — just different ways of presenting them (see Akaike 1969, for demonstration of (i) and (ii); Yates and Goodman 2005 for proof of equivalence for (ii) and (iii)).

In the past decades, many techniques and algorithms have been developed for understanding various features of complex systems such as brain electrical activity. In particular, a variety of nonlinear dynamical measures has been applied to EEG

recordings and received extensive attention for the new information they derived in various physiological and pathological studies. Nonlinear measures such as marginal predictability, phase coherence, Lyapunov exponents, similarity index, mutual information and effective correlation dimension, offered important understanding of nonlinear dynamics in brain functions in focal epilepsy and Alzheimer's disease (see, for example, Li et al., 2003a; Zhang et al., 2009a; Mormann et al., 2000; Lehnertz et al., 2000; Le Van Quyen et al., 2000; Jeong et al., 2001; Jeong 2002).

The nonlinear content in time series can be tested explicitly with the method of surrogate data (Schreiber and Schmitz, 2000). In this algorithm, a Fourier transformation of the original time series is performed and a "linear surrogate data set" is generated by randomization of the phase profile. The new surrogate data should preserve the same linear properties of the original time series without adding any nonlinear structure to the data. For any nonlinear metric of interest, comparisons are conducted between the original data set and a collection of the linear surrogate data sets, which is collected by repeating the randomization for a number of times. One simple measure that is used to determine whether the value of the metric on the original data is substantially different from its typical value on the surrogate data is defined by

$$\Phi = \frac{|V_o - \bar{V}_s|}{\sigma_S(V)} \tag{1.1}$$

where V_o is the value of the metric on the original data, $\bar{V}_s$ is the mean of the values of V computed on the surrogate data, and σ_S is the standard deviation of those

values. Values of Φ greater than 3 are generally considered to be significant in the values of V on the original and surrogate data.

Many studies have shown the existence of nonlinear structure in EEG recordings. For example, the null hypothesis that there is nonlinear structure in scalp epileptic EEG data was tested by Li et al., 2003b. The authors performed the surrogate data method on 94 20-minute epileptic EEG epochs, in which they found a clear difference between the original and the surrogate data sets, which indicated nonlinear structures in the scalp EEG data. Stam et al., 1995 and Jelles et al., 1999 also used surrogate data methods to analyze properties of nonlinearity in EEG from patients with Alzheimer's disease. For more detailed discussion about the physical-mathematical theory of nonlinear dynamics, see Schuster 1989 and Ott 1993.

1.2 Nonlinear Metrics vs. Linear Metrics

In the previous section, we mentioned several nonlinear metrics that are sensitive to the nonlinear structure in a time series. However, it is not clear whether these nonlinear measures are more informative than the three simple linear measures. From a practical point of view, a less computationally intensive measure is preferred for developing a reliable ambulatory method in studies of time series analysis. It is important to determine whether nonlinear metrics are more appropriate than linear metrics, since the linear metrics are in general simpler in both computation and interpretation. Therefore, comparing the performance of linear and nonlinear metrics on the same data set is desired to explore the extent to which nonlinear

metrics can offer over the linear metrics.

For this purpose, Li et al., 2003b studied the performance of two linear measures, standard deviation and the 1st order coefficient of an autoregressive model (σ^2 and a_1), using epileptic scalp EEG data. In their study, σ^2 and a_1 were computed for 94 20-minute scalp EEG epochs. A linear regression model was implemented to test for temporal correlation between epileptic seizure onset and the linear metrics computed for both the original time series and surrogate data. The same set of statistical methods was repeated for a nonlinear metric (marginal predictability). Their results indicated statistically significant difference between the original time series and surrogate data by using the nonlinear metric, and failure to reject the null hypothesis (no difference between the original time series and the surrogate data) by using linear metrics. In this thesis, we continue to study the properties of nonlinear dynamics in scalp EEG by using phase coherence, and use an example of scalp EEG recordings from patients with Alzheimer's disease to show that a nonlinear dynamical metric (phase coherence) is more effective than a linear metric (cross correlation) as a biomarker.

1.3 Marginal Predictability

With the realization that nonlinear dynamics was embodied in brain electrical activity, many studies were carried out with the development of new nonlinear dynamical metrics. Among many others, Savit and Green 1991 (also see Wu et al., 1993) proposed a nonlinear metric called "marginal predictability" based on the

correlation integral:

$$C_d(y(i), y(j)) = P(\| y^{(d)}(i) - y^{(d)}(i) \| < \varepsilon) \tag{1.2}$$

where *P(.)* is the probability of the argument, x_j is the *jth* element of the time series, $y^{(d)}(i)=(x_i, x_{i-1}, \ldots, x_{i-d-1})$ is a *d*-dimensional vector from the data. The notation ||.|| is the max norm of the argument.

The quantity C_d measures the probability of two *d*-dimensional vectors from the time series being close to each other, within a certain distance ε. In other words, it measures the likelihood of two sequences of length d taken from the data to be similar to each other. Predictability (Savit and Green, 1991) is then defined as

$$S_d = \frac{C_{d+1}}{C_d} \tag{1.3}$$

which can also be interpreted as the conditional probability $P(z_{d+1}|z_d, \ldots, z_1)$.

Although S_d can be used directly as a nonlinear statistic, (Manuca and Savit, 1996) found a more sensitive discriminator of nonlinear structure in time series, which is defined as

$$R_d = \frac{S_d}{S_{d-1}} = \frac{C_{d+1}C_{d-1}}{C_d^2} \tag{1.4}$$

To make the interpretation simple, the marginal predictability is defined as

$$\delta_d = \frac{R_d - 1}{R_d} \tag{1.5}$$

δ_d measures the additional predictive information in the *(d+1)st* lag of the time series, conditioning on the information already known in the previous d lags. If δ_d is close to zero, then little predictive information is added to the current knowledge of the time series by using d lags. If δ_d is significantly different from zero, then there is substantial predictive information in the *(d+1)st* lag.

There are two major reasons that we introduced the mathematical background of marginal predictability in this section. First, marginal predictability is a nonlinear metric derived from the definition of correlation integral. Correlation integral is not only one of the most important and basic nonlinear measure, but also the foundation of many other nonlinear metrics, such as effective correlation dimension and the similarity index (see 1.5 for more details). Correlation integral can also be used in the BDS test, to detect the *I.I.D.* (independent identical distributed) assumption of a time series (Brock et al., 1987). The second reason is that, studies in marginal predictability described a general structure of long-distance connection over different parts of the brain, which is essential in understanding the nonlinear dynamics of the brain function in neurological diseases. In these studies, marginal predictability was shown to be correlated with the conditions that allow (or promote) the spread of paroxysmal neural activity from the seizure focus to more distant parts of the brain, and correlated with the time to a seizure for patients with temporal lobe epilepsy (Li et al., 2003a, 2003b, 2006; Drury et al., 2003). In their studies, differences in the values of MP between two electrodes were computed for different pairs. It was found that this difference computed for two electrodes, one near the seizure focus and

one distant from it (generally an occipital electrode ipsilateral to the side of the seizure focus) was large during interictal periods (defined as at least two hours away from any seizure) but decreased, typically several tens of minutes prior to a seizure. Interestingly, similar calculations performed on normal control subjects indicate a small value of the difference of MPs, so that, by this metric, the brains of people with epilepsy start to look more normal as a seizure approaches, than they do interically.

In particular, closer values of MPs from two electrodes indicate that the signals from these electrodes are more similar, in some sense, than they would be if the MPs had very different values. This suggests some increased ease of communication between the regions of the brain recorded by those electrodes. Such an increase in the epileptic brain's ability to communicate (or transfer information) across long distances could facilitate the development of a seizure, in that it could more easily allow the paroxysmal activity near the seizure focus to spread to distant parts of the brain. The fact that differences in the MPs are greater, interictally than corresponding differences in normal subjects further supports this picture: The idea is that the epileptic brain, in the interictal state manages to functionally isolate the seizure focus, and by that isolation inhibit propagation of paroxysmal activity across the brain. When that inhibition breaks down, full blown seizures are allowed to develop.

1.4 Phase Coherence

Although the marginal predictabilities are somewhat abstract, previous studies do

suggest a qualitative story concerning the spread of paroxysmal activity beyond the region of the seizure focus. To further explore this picture, phase coherence between the signals from pairs of scalp electrodes has been used to study neuronal information processing and long distance communication between different areas of the brain (Bhattacharya, 2001; Mormann et al., 2000). In addition to being sensitive to dynamical effects, phase coherence has the advantage of being more popular than marginal predictabilities. For example, phase coherence can be studied in different frequency bands. This is very useful since there has been some work on the role of different frequencies in long distance information transfer in the brain (Kopell et al., 2000).

In the following we introduce the mathematical background of phase coherence.

1.4.1 Hilbert Transform

The phase profile of a time series *x(t)* can be obtained from the corresponding complex signal:

$$X(t) = x(t) + ix_h(t) = x(t) + i\frac{1}{\pi}\int_{-\infty}^{\infty}\frac{x(\tau)}{t-\tau}d\tau \tag{1.6}$$

where $x_h(t)$ is the Hilbert transform of the original signal *x(t)*. The instantaneous phase is then

$$\varphi(t) = arg(x_h(t)/x(t)) \tag{1.7}$$

where $-\pi \leq \varphi(t) \leq \pi$. Strictly speaking, the definition of phase is only meaningful for narrow-band signals (although some authors do study "broad-band" phase coherence, see Dominguez et al., 2005; Mormann et al., 2000; Mormann et al., 2003; Ponten et

al., 2007).

Since the Hilbert transform is equivalent to a convolution of the time series with $\frac{1}{\pi}P(\frac{1}{t})$, whose Fourier transform is a step function, phase *φ(t)* is also the phase associated with the original time series *x(t)*. Therefore a specific phase can be determined at any time for this time series (Bendat and Piersol 2000).

1.4.2 The Wavelet Transform

Another method to extract the phase profile of a time series is to use the complex coefficient of its wavelet transform:

$$W_x(t;\omega) = \int_{-\infty}^{\infty} x(u)\Psi^*_{t,\omega}(u)du \tag{1.8}$$

where $\Psi^*_{t,\omega}(u)$ is the complex conjugate of the Morlet wavelet defined at time *t* and frequency ω by:

$$\Psi^*_{t,\omega}(u) = \exp[i\omega(u-t)]\exp[-\frac{(u-t)^2}{2\sigma^2}] \tag{1.9}$$

Then the phase profile is the angle of the complex coefficient:

$$\phi(t) = \arg[W_x(t;\omega)] \tag{1.10}$$

Wavelet transform has the advantage that it does not require pre-filtering since a choice of appropriate wavelet would suffice it. If the chosen wavelet $\Psi^*_{t,\omega}(u)$ is analytic, then the complex coefficient $W_x(t;\omega)$ would also be analytic. Therefore a definite phase can be defined since analytic signals do not have negative frequency components. However, if the center frequency of interest is high enough, wavelet transform may suffer from difficulties since the number cycles would be extremely high. In our study, we computed the phase profile with both methods and found

their results to be qualitatively similar. Hence we only used Hilbert transform. For more details on the background about phase coherence and comparing these two methods, please refer to (Le Van Quyen et al., 2001; Rosenblum et al., 2001).

1.4.3 Phase Profile and Phase Coherence

For a pair of signals $x_1(t)$ and $x_2(t)$, instantaneous phases of each signal are calculated according to Eq. (1.7) and phase differences are defined to be

$$\Delta\phi = |\phi_1 - \phi_2| \, mod \, 2\pi. \tag{1.11}$$

In order to characterize phase coherence between the two signals, an index based on Shannon's entropy of the phase differences is computed as follows (Tass et al.,1998)

$$\rho = \frac{H_{\max} - H}{H_{\max}} \tag{1.12}$$

where the entropy is

$$H = -\sum_{i=1}^{M} p_i \ln p_i \tag{1.13}$$

M is the number of bins used to obtain the distribution function, and p_i is the probability of finding the phase difference within the i-th bin. The maximum entropy ($H_{\max}$) is given by lnM; the optimum number of bins M is set as $e^{0.626+0.4ln(L-1)}$ where L is the length of the data (Otnes and Enochson, 1972). The values of ρ are bounded between 0 and 1. It measures the synchronization of cellular activities in the brain and reflects the complexity of cortical dynamics. Large values of phase coherence between two EEG electrodes correspond to good communication in the

brain.

Other related metrics, such as the phase locking value (PLV) are also used commonly to characterize the degree of phase coherence. However, PLV and ρ often have quite similar profiles and lead to similar conclusions (Zhang et al., 2009a). Therefore, in this analysis we will present results only for ρ.

1.5 Other Nonlinear Metrics

In the past decades, many other nonlinear dynamic metrics have also been extensively studied to better understand the different states of brain function. For example, estimates of an effective correlation dimension D_2^{eff}, have been shown to characterize features extracted from epileptic intracranial EEG (Lehnertz et al., 1998; Lehnertz et al., 2001). The results of this time-resolved analysis indicated changes in nonlinear characteristics, in particular, decreases in D_2^{eff} for up to several minutes prior to seizure onsets. These authors also found that the maximum synchronization S_σ and S_τ, defined as the maximum deflection from an upper threshold T_u which was determined by D_2^{eff} and the duration with D_2^{eff} below T_u respectively, showed potential capability to predict epileptic seizures.

Le Van Quyen et al., 1999 proposed another nonlinear methodology, the similarity index γ, also based on the correlation integral (see definition in 1.3). Their analysis of intracranial brain activities showed a 'preictal phase' preceding the epileptic seizure. In particular, they reported significant decreases in the similarity index during seizure onset, and a potential seizure anticipation period several minutes

in advance (Le Van Quyen et al., 2000).

Other nonlinear dynamic metrics that are worth mentioning include Lyapunov exponent and mutual information. Lyapunov exponent has been used extensively in studies of nonlinear dynamics in brain electrical recordings from Alzheimer's disease. Stam et al., 1995 and Jeong et al., 1998 showed decreased complex brain activity in patients with AD compared with age-matched normal subjects. Since Lyapunov exponent can also be understood as a measure of flexibility of brain function, it is believed that decreases in Lyapunov exponent in AD patients indicate a drop in information processing capability in AD brains (Jeong 2002). Mutual information (MI) has also been widely used for detecting nonlinear dependencies between time series. Xu et al., 1997 investigated cross mutual information among 8 EEG electrodes and described information transmission among different cortical areas in sleeping and awake states. Jeong et al., 2001 analyzed MI of scalp EEG data from 15 AD patients, and found lower level of information transmission between frontal and antero-temporal regions.

1.6 Summary

With the renaissance of nonlinear dynamics in the past decades, there have been extensive studies that explore the nonlinearities embodied in many natural processes. Brain electrical activity, and specifically EEG was no exception (Duke and Pritchard 1991). In this chapter, we showed that it is necessary to use nonlinear dynamical methods in the analysis of EEG recordings, and introduced several nonlinear

measures that have been proved useful in understanding brain dynamics. In particular, studies in epilepsy suggested increased ease of communication between the distant regions of the brain prior to a seizure onset. Such an increase in the epileptic brain's ability to transfer information across distant regions of the brain could lead to the development of a seizure. For Alzheimer's disease, patients exhibit reduced nonlinear dynamics in the EEG compared with normal subjects, indicating decreased complexity in brain electrical activity. However, most nonlinear metrics mentioned in this chapter (except for phase coherence) are only studied for the broad band EEG data. It would be extremely beneficial to have a detailed study that investigates both the spatial and frequency domain of the EEG data. Given the advantage that phase coherence can be applied to signals of different frequency bands, we conducted advanced statistical models to study the nonlinearities of brain dynamics for two neurological diseases (temporal lobe epilepsy and Alzheimer's disease) in chapter 2 and 3. We will demonstrate that phase coherence is correlated with both spatial and temporal precursors of epileptic seizures in the scalp EEG data, and show that it is more effective than a linear measure (cross correlation) as a biomarker in a pilot study of scalp EEG from Alzheimer's disease.

CHAPTER 2

PREICTAL CHANGES IN PHASE COHERENCE FROM SCALP EEG IN TEMPORAL LOBE EPILEPSY

2.1 Introduction

2.1.1 About Epilepsy

Epilepsy is a common chronic neurological disorder that affects 2.5 million people in the US, with about 150,000–200,000 new cases diagnosed per year (Begley et al., 2000). The occurrence of episodic seizures is the most distinguished feature of epilepsy, which usually results to the dangerous and embarrassing consequences, and the anxiety and pressure associated with the uncertainty of seizure occurrence. There are basically two types of epilepsy, focal and generalized. Over 50% of all epilepsy cases are focal epilepsies, in which seizures originate in a focal region and spread to other parts of the brain. In generalized epilepsy, seizures cannot be clearly identified for their site of origination. The most common type of focal epilepsy is temporal lobe epilepsy (TLE), in which seizures begin in one or both temporal lobes of the brain. To be more specific, mesial temporal lobe epilepsy (MTLE) arises in the hippocampus, amygdale and parahippocampal located in the inner aspect of the temporal lobe; lateral temporal lobe epilepsy (LTLE) arises in the neocortex on the outer surface of the temporal lobe of the brain. In the majority of epilepsy patients, seizures can be controlled with medical or surgical treatments. However, 20-30% of

focal epileptic patients are refractory to all forms of medical therapy. Therefore, understanding the dynamics of epileptic seizures has become a key to understanding, preventing and curing medically refractory epilepsy.

2.1.2 Nonlinear Dynamics in Epileptic EEG

A key question in understanding the dynamics of seizures concerns the spread of the seizure from the focal region to other parts of the brain. Previous studies (Li et al., 2003a, 2003b) suggest that the conditions that allow (or promote) the spread of paroxysmal neural activity from the seizure focus to other parts of the brain may presage a seizure by up to an hour or so. Several human and experimental studies also supported the evidence of a transition phase which is up to one hour before the seizure onset. For example, in a recent human study, increased blood flow was detected in the epileptic temporal lobe for about 10 minutes before the seizure onset (Weinand et al., 1997). An epidemiologic investigation also found prevalence of clinical prodromes in over 50% participating patients (Rajna et al., 1997). A time-frequency mapping method demonstrated systematic changes in the R-R interval on ECG of TLE patients, which could be events associated with seizure precursors (Novak et al., 1999). Blood flows in the cerebral epileptic and non-epileptic cortex were also found to become positively correlated about 10 minutes prior to seizure onset, which is opposite to their negative correlations in interictal periods (Gonzalez-Portillo et al., 2004).

To better answer this question, researchers have started searching for

independent features and patterns that may herald epileptic seizure since the early 1970s. Up to now, it has been well understood that brain activity, as a result of a large number of cellular activities, could be modeled as a nonlinear dynamic system (Iasemidis et al., 1988; Lehnertz and Elger, 1998; Lehnertz et al., 2001). In the past decades, various studies have investigated nonlinear dynamical methods to analyze epileptic EEG data (Mormann et al., 2000; Lehnertz et al., 1995; Le van Quyen et al., 2000).

The ability to predict epileptic seizure onset would be a great benefit to many people with epilepsy. While attempts at seizure prediction have so far been largely unsuccessful, it is generally believed that many seizures are preceded by a preictal period which may last as long as a couple of hours prior to a seizure (Schindler et al., 2001; Li et al., 2003a; Mormann et al., 2003; Zhang et al., 2009a). Understanding the nature of this preictal period and the changes in neural dynamics that accompany it, is important not only to the development of a robust seizure prediction method, but also to a deeper understanding of ictogenesis, and the therapeutic benefits that will follow that understanding.

Phase coherence is such a nonlinear dynamic metric which can be used to study neuronal information processing and long distance communication between different areas of the brain (Bhattacharya, 2001; Mormann et al., 2000). In addition to being sensitive to somewhat different dynamical effects, this metric has the advantage of being more familiar than are marginal predictabilities. Moreover, phase coherence can be studied in different frequency bands. This is useful since there has been some

work on the role of different frequencies in long distance information transfer in the brain (Kopell et al., 2000). To further explore this picture, we will study the phase coherence between the signals from pairs of scalp electrodes.

As we shall show, our study of phase coherence is consistent with the general picture of increased communication between widely separated regions of the brain, including (but not necessarily limited to) the seizure focus at least tens of minutes prior to a seizure. More importantly, we continue our study of data from scalp EEG with a particular focus on the preictal period, and investigate the long-distance communication interictally in the brains of epileptics compared to normal subjects.

2.2 Subject Selection

For this study, we used scalp EEG data that were collected from 17 patients (mean age 42.9 years, standard deviation, 11.2 years range 23 – 63 years of age) with MBTLE. Patients were admitted to the long term monitoring unit of the Henry Ford Hospital in Detroit, during which spontaneous partial seizures were recorded. Patients were evaluated by an epileptologist, who followed a standardized protocol (Valachovic 1997) of presurgical evaluations, which is similar to such assessments at most major epilepsy centers. In an effort to provide as homogeneous and therefore comparable a group of patients as possible, we have limited our analysis to patients with medically refractory mesiobasal temporal lobe epilepsy, the most common patient group considered as suitable candidates for epilepsy surgery. The specific criteria for inclusion in our analysis are:

1. Seizures had to be of unilateral mesiobasal temporal lobe origin, documented by history, interictal and ictal EEG recordings.

2. Age between 23 and 63 years. This reduces the likelihood of age related disorders such as cerebrovascular disease.

3. No mass lesion detected with magnetic resonance imaging (MRI) technology.

4. Intelligence Quotient of 70 or more.

5. No evidence of a progressive neurological disorder, active neurological disorder other than epilepsy, and no other significant medical disorder, severe depression or psychosis.

6. No evidence of damage to the hippocampus contralateral to the seizure focus as determined by MRI.

7. No history of drug or alcohol abuse.

8. Patients receiving barbiturates or benzodiazepines were excluded with the exception of intravenous benzodiazepines used for acute seizure control.

9. No history of drug use other than antiepileptic drugs during the two weeks prior to the recordings.

Patients admitted to such long term monitoring units typically are undergoing or have undergone withdrawal from antiepileptic drugs. Although this withdrawal may increase seizure frequency, we do not believe that it affects the kinds of relationships between interictal and preictal electrographic metrics that we study. However, one must recognize that any use of data from long term monitoring units is subject to this potential confound. Furthermore, no systematic electrographic difference was found

based on etiology in the given MBTLE subjects. In addition to data from patients in the long term monitoring unit, we used data that were collected from five non-epileptic subjects (age range 24-34). Normal subjects had no history of drug and alcohol abuse, and had not used any medications in the two weeks prior to the study. Although age and sex are not precisely matched between epileptic patients and normal subjects, there is no obvious sex difference in scalp EEG and the ages of all participants fall into the range between 23 - 63 years where little electrographic difference is generally observed.

2.3 EEG Data and Control for Behavior States

It is well recognized that seizures during sleep tend to occur preferentially during stage 2 sleep. On the other hand, even absent an impending seizure, there is no *a priori* reason to suppose that stage 2 sleep necessarily has the same phase coherence characteristics as other behavior states. One might, therefore, be concerned that our observations of an overall increase in phase coherence preictally is entirely attributable to the prevalence of stage 2 sleep preictally. Therefore, for this study, we will discuss the effects of behavior states in much greater detail.

We used scalp EEG data that were collected from 17 patients with MBTLE, who were admitted to the long term monitoring unit of the Henry Ford Hospital. EEG were recorded on a 128-channnel BMSI/Nicolet 5000 System sampling at 200Hz. The band pass was .5 Hz to 100 Hz. The digital data was transferred to UNIX workstations for conversion to ASCII text data and further analysis. There were a

total of 26 scalp electrodes placed according to the standard 10-20 International system (Jasper 1958). To eliminate spatial overlap, 16 electrodes of interest were selected for analysis (excluding central electrodes Fz, Cz and Pz). A sketch of electrode placement is shown in Fig. 2-1.

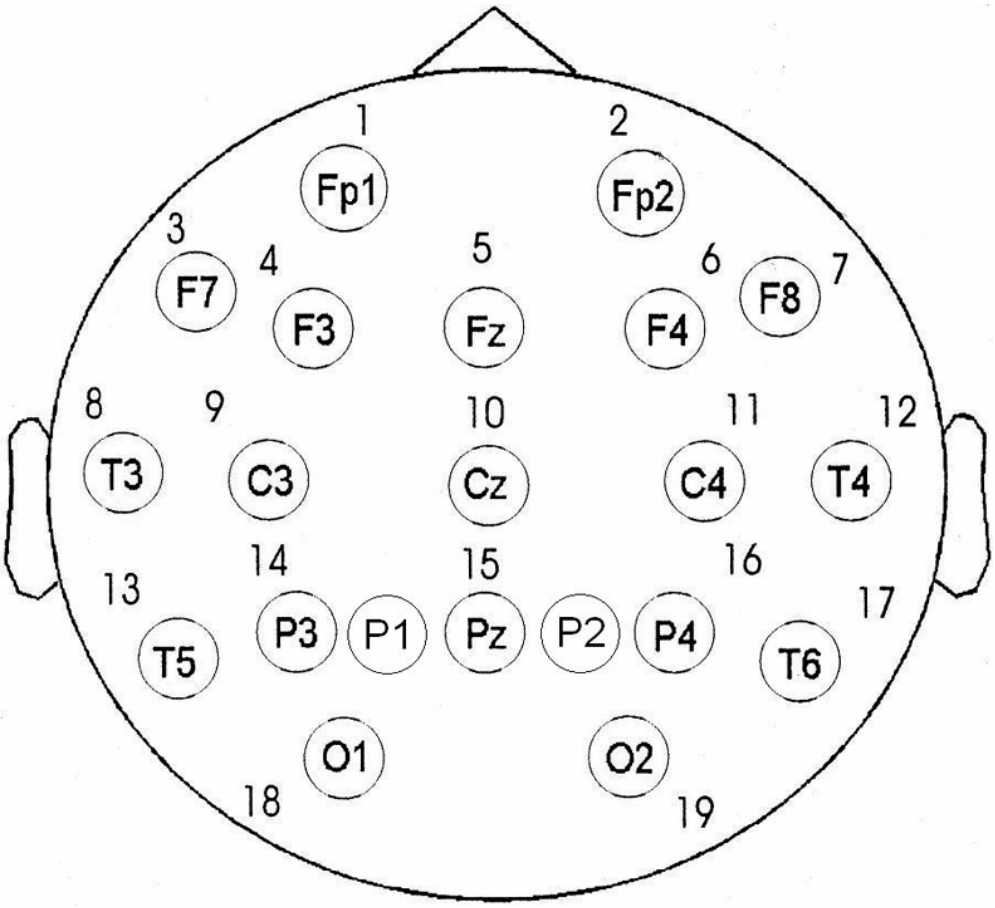

Figure 2-1. Scalp EEG electrode placement.

The EEG data were examined by a board certified epileptologist who noted the times of seizure onset, as well as the behavior state of the subject (see below). Because EEG data differs markedly depending on behavior state, it was important to control for this variable. The EEG were scored and subject behavior state for each 10-minute interval was placed into one of the following categories:

Awake, eyes open or closed—AEO, AEC

Drowsy, lightly or heavily —D1, D2 and sleep state S1 (In the sequel, these states will be referred simply as S1.)

Sleep state S2

Sleep state, (slow wave sleep) S3/S4

REM sleep – REM

We also pre-filtered the data by eliminating the epochs with a substantial amount of artifact. From the remaining EEG, 1 – 3 epochs of two hours length were randomly selected from each subject. Each two hour epoch was catalogued as either preictal, for which a seizure occurred at the end of the interval, or interictal for which there were no seizures within two hours of the beginning of the interval or two hours from the end of the interval. The two hour epochs were further divided into 12 10-minute intervals. Each 10 minute interval was scored for behavior state according to the dominant state exhibited in that interval. Thus, each 10 minute interval carried both a label for the dominant behavior state as well as a label describing the proximity (interictal or preictal) of that interval to the nearest seizure. In total, 26 two-hour interictal and 30 two-hour preictal epochs were used. In the 30 two hour preictal epochs there were a total of 179 AEO or AEC intervals as well as 66 S1, 82 S2, 19 S3/S4, and 14 REM intervals. Among the 26 two hour interictal epochs there were 133 AEO or AEC intervals as well as 57 S1, 99 S2, 10 S3/S4, and 13 REM intervals. (Note that, for example, a 10 minute preictal sleep interval may have preceded a seizure occurring, at the end of the two hour epoch from which that interval was drawn, in an awake state.) The proportions of intervals with different

behavior states associated with preictal epochs are not the same as the proportions associated with interictal epochs (chi-square p=0.001). This, however, is irrelevant for our model controlling for behavior states, because statistical models were implemented separately for each behavior state.[1]

2.4 Reference Electrode

Another important issue to address with respect to the computation of phase coherence is the problem of the reference electrode. In EEG, voltage differences are recorded, which means that the time series associated with an electrode is really the time series of the voltage difference between that electrode and a reference electrode. For the data used here, the common reference voltage is an average of leads, P1 and P2, which are located to either side of Pz. Guevara et al., (2005) has shown that the interpretation of phase differences between two electrodes can, as a matter of principle, be problematic depending on the behavior of the (common) reference electrode. To address this potential problem, we recomputed our results using the central electrode, Cz, as the reference. There are quantitative differences in the results between the two different reference schemes. However, the qualitative picture of preictal phase coherence increase in anterior electrodes, as well as the importance of the β_2 band is supported by both reference schemes. We are therefore reasonably confident that our qualitative conclusions are not affected by reference

[1] For Wilcoxon rank-sum test and the spatial model without controlling for behavior states, a smaller data sample with more balanced behavior states is used.

problems.

2.5 Statistical Methods

2.5.1 Wilcoxon Rank-Sum Test and Spatial Distribution Models without Controlling for Behavior States

For the 16 electrodes shown in Fig. 2-1, there are a total of 120 possible pairs of electrodes. In this section, we divided all 120 electrode pairs into two general groups (long-range or short-range) based on the location of the electrodes. A long-range pair is one in which the two electrodes are either located in opposite hemispheres, or are not immediate spatial neighbors (e.g. P_7-C_3 is considered a long-range pair). A short-range pair is one in which the two electrodes are neighboring and in the same hemisphere. These definitions were, to our knowledge, first suggested in (Bhattacharya, 2001). With these definitions we consider phase coherence for several different cases.

Case I: Phase coherence among long-range pairs (98 pairs).

Case II: Phase coherence among short-range pairs (22 pairs).

Based on the discussion in the Introduction, long-range coherence involving focal electrodes (scalp electrodes adjacent to the seizure focus) may be of special interest. Therefore, we also study the following categories of electrode pairs:

Case III: Homologous pairs in which one electrode is adjacent to the seizure focus.

Case IV: Long-range pairs in which one of the electrodes is adjacent to the seizure focus (23 pairs). This is a subset of the pairs considered in Case I.

We are interested in assessing, in each of these cases, how phase coherence depends on the state of the system, i.e. whether the data was taken from an interictal or preictal epoch, or from a normal, non-epileptic subject. To that end, we computed phase differences between pairs of electrodes in each band, and the mean phase coherence (ρ) values for each band and electrode pair for 20 second windows. (Note that sampling at a lower frequency does not materially affect our results.) The 20 second windows were chosen with four second overlaps, so that one two hour epoch consists of 450 windows. (This choice of windowing and overlap was also useful for the regression analysis, below.) The average value of ρ was then computed for each two hour epoch. Within each band, and for each electrode pair, we then compared those two hour average values between pairs of states (interical, preictal or normal) to see if there was a statistically significant difference in the average phase coherence among the states. The coherence values between pairs of states were compared statistically by one-tailed non-parametric Wilcoxon rank-sum test ($p \leq 0.05$). (See Appendix 1 for an introduction to Wilcoxon rank-sum test.) For a given pair of states (interictal/preictal, interictal/normal, preictal/normal), three counters were created for possible outcomes for each pair of electrodes in each window: 1) stronger coherence in first state, 2) stronger coherence in second state and 3) no statistically significant difference between the two states. For cases I, II, and IV (multiple pairs) we tallied the number of electrode pairs falling into each of the above three categories and incremented the corresponding counters. Case III was not included in the Wilcoxon analysis since there is only one electrode pair being studied, but is included

in our regression analysis.

In addition to Wilcoxon test, the linear mixed model (see Appendix 2) was performed to the same dataset for two reasons. First, while we should not, typically, expect to see any temporal dependence of our results as we move through a two hour epoch of interictal or normal data, there may be some temporal dependence during the two hour preictal epoch. Such temporal dependence can be included in a regression analysis. Second by including a state variable that distinguishes between interictal, preictal and normal states, we can introduce another statistical method for assessing the dependence of phase coherence on the state. As we shall see, the results of this alternative analysis are largely consistent with our Wilcoxon results, but do provide a different perspective on the relationship between phase coherence and state. The response variable in our regression analysis is the phase coherence measure (e.g. ρ) and covariates include time (measured by 10-minute windows) and the state indicator of that time window. In order to account for the temporal dependence of phase coherence in different windows, we adopted linear mixed models with random intercept. The significance level in the analysis was set to $p \leq 0.05$.

2.5.2 Spatial Models with Controlling for Behavior States

Since it is well observed that behavior states plan an important role in brain dynamics preceding an epileptic seizure during sleep (e.g. seizures tend to occur preferentially during stage 2 sleep), we categorized the scalp EEG data according to the criterions in section 2.3. Statistical models were then implemented separately for

each behavior state. In the following we present four linear mixed models. Each of these models can be applied to data filtered in different frequency bands. The dependent (response) variable in our models is the phase coherence measure, ρ, and the covariates are selected from seizure state and location of electrode. We are primarily interested in determining how differences in phase coherence between interictal and preictal states depend on spatial location, and, in particular, between anterior and posterior pairs of electrodes, and between ipsilateral and contralateral pairs. To simplify our description, the location of an electrode will be denoted by two letters: A or P for anterior or posterior and I or C for ipsilateral or contralateral to the seizure focus. So, for example, the location of an anterior electrode contralateral to the site of the seizure focus will be denoted by AC.

The variables and models presented below are designed to compare the larger scale structure of phase coherence that distinguishes entire halves of the brain (anterior vs. posterior, or ipsilateral vs. contralateral). Generally, we have not addressed the more detailed question of the behavior of pairs of electrodes all of which are contained within a one-quarter segment of the brain. (E.g. both electrodes of the pair having the location PI.) An exception to this is an analysis of anterior (posterior) electrode pairs which are short-range, in the sense that both anterior (posterior) electrodes are in the same hemisphere of the brain (E.g., both electrodes of the pair are AI or are AC.). We have also done a separate analysis of those anterior (posterior) electrode pairs which connect the two halves (ipsilateral to contralateral) of the brain. (E.g. one electrode is AI and one is AC. See Section III for more

details.) In addition, we have included one model (model 3), with which we compare interictal vs. preictal phase coherences on pairs of electrodes that cross the brain diagonally, so that one member of the pair is AC and the other is PI, or one member is AI and the other PC.

In constructing these models, the following dummy variables were created to implement these covariates:

L_1=1 if both electrodes are anterior (FP1, FP2, F3, F4, F7, F8, T3, T4, C3, C4) and L_1=0 if both electrodes are posterior (T5, T6, P3, P4, O1, O2)

L_2=1 if both electrodes are posterior and L_2=0 otherwise

C_1=1 if both electrodes are ipsilateral (located in the same hemisphere of seizure focal region) and C_1=0 otherwise

C_2=1 if both electrodes are contralateral (located in the opposite hemisphere of seizure focal region) and C_2=0 otherwise

D_1=1 if one electrode is ipsilateral anterior and the other electrode is contralateral posterior and D_1=0 otherwise

D_2=1 if one electrode is ipsilateral posterior and the other electrode is contralateral anterior and D_2=0 otherwise

G_1=1 if the epoch is preictal and G_1=0 otherwise

G_2=1 if the epoch is interictal and G_2=0 otherwise

Within each frequency band and for each behavior state, there were 37 phase coherence values (associated with 20 second windows) for each 10-minute interval from each of the 30 two hour preictal epochs and the 26 two hour interictal epochs.

The following models and statistical tests were applied to estimate the effects of temporal proximity to seizure (i.e., preictal or interictal) and electrode pair location for each frequency band and behavior state. (Clearly, the set of electrode pairs used is different for different models. See the next section for more details.)

Model 1: mean phase coherence as a function of seizure state (globally for all pairs):

$$\rho = a_0 + a_1 G_1 \tag{2.1}$$

Null hypothesis $a_1=0$, alternative hypothesis, $a_1\neq 0$.

Model 2: mean phase coherence as a function of electrode pair location such that both members of the pair are anterior ($L_1=1$) or both member of the pair are posterior ($L_2=1$) and seizure state (interictal or preictal).

$$\rho = a_0 + a_1 L_1 + G_1 \sum_{i=1}^{2} b_i L_i \tag{2.2}$$

Null hypothesis $a_1=b_1=b_2=0$, alternative hypothesis, $a_1\neq 0$ or at least one of the b_j (j=1.2) is non-zero.

Model 3: mean phase coherence as a function of seizure state (interictal or preictal) and electrode pair location such that one member of the pair is anterior and the other is posterior, but both are either ipsilateral ($C_1=1$) or contralateral ($C_2=1$) to the seizure focus.

$$\rho = a_0 + a_1 C_1 + G_1 \sum_{j=1}^{2} b_j C_j \tag{2.3}$$

Null hypothesis $a_1=b_1=b_2=0$, alternative hypothesis, $a_1\neq 0$ or at least one of the b_j (j=1.2) is non-zero.

Model 4: mean phase coherence as a function of seizure state (interictal or preicta) and electrode pair location such that one member of the pair is anterior and

contralateral (AC) to the seizure focus and the other member is posterior and ipsilateral (PI) to the seizure focus (D_1=1) or such that one member of the pair is anterior and ipsilateral (AI) to the seizure focus and the other member is posterior and contralateral (PC) to the seizure focus (D_2=1):

$$\rho = a_0 + a_1 D_1 + G_1 \sum_{j=1}^{2} b_j D_j \qquad (2.4)$$

Null hypothesis $a_1=b_1=b_2=0$, alternative hypothesis, $a_1 \neq 0$ or at least one of the b_j (j=1.2) is non-zero.

2.6 Results

2.6.1 Spatial Distribution Models

2.6.1.1 Wilcoxon Rank-Sum Test

We first present our results using the Wilcoxon analysis described above for Cases I, II and IV. We will then present the results of our regression analysis. For completeness, we will present our results using each of our different reference electrodes, (P_1+P_2) and C_z. In the discussion section we will comment on the differences in these results.

Normal vs. Interictal and Preictal states

We first examine the difference in phase coherence between normal subjects and patients with epilepsy for both the interictal state and preictal state. To that end, refer to Fig. 2-2a and 2-2b. Each of these figures represents the results of our Wilcoxon analysis using a different reference electrode. Fig. 2-2a and 2-2b uses reference electrode (P_1+P_2) and C_z, respectively. In each figure we plot three bar

graphs corresponding to cases I (all long range pairs), II (all short range pairs) and IV (all long range pairs with one electrode being a focal electrode), as described above. In each graph we plot the percentage of pairs in that case for which the average phase coherence is statistically larger in normal subjects compared to the interictal state (blue bars) or the preictal state (red bars) . The percentage of pairs for which the average phase coherence is statistically *lower* in normal subjects compared to the phase coherence in either the interictal or preictal state for epileptic subjects is negligible (average 2.4%, range 0-13%) for all cases and frequency bands of all three references.

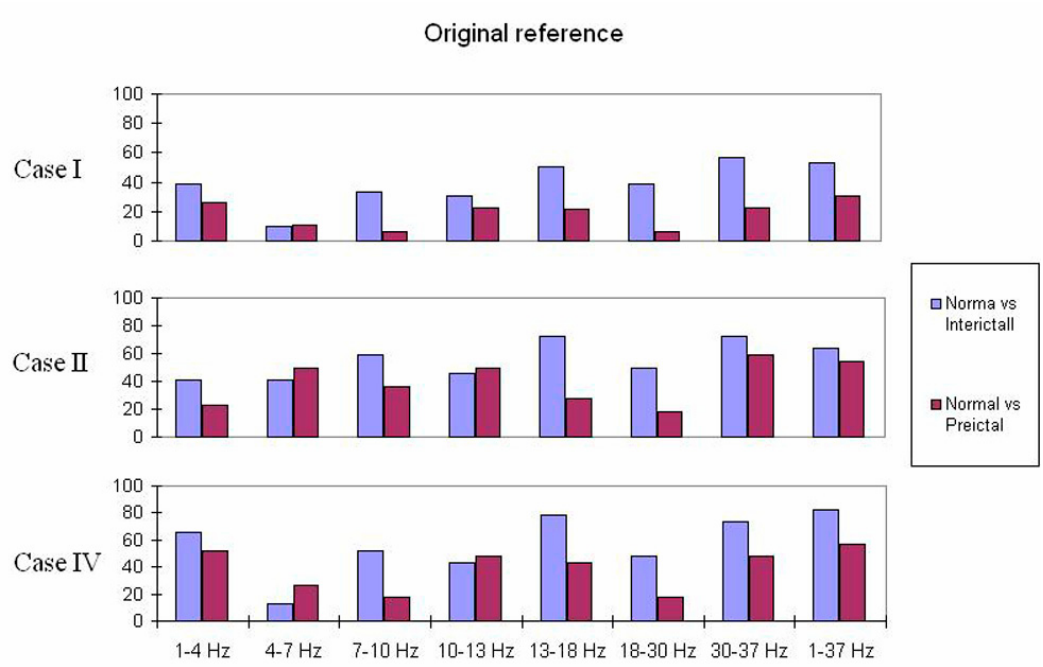

Figure 2-2a. Wilcoxon test results for phase coherence in normal vs. interictal epochs and in normal vs. preictal epochs using reference electrodes (P_1+P_2). Blue bars indicate the percentage of pairs for which the phase coherence is larger in the normal state than the interictal state, and red bars indicate the percentage of pairs for which the phase coherence is larger in the normal state than the preictal state.

Figure 2-2b. Wilcoxon test results for phase coherence in normal vs. interictal states and in normal vs. preictal states using reference electrode C_z. Blue bars indicate the percentage of pairs for which the phase coherence is larger in the normal state than the intericatal state, and red bars indicate the percentage of pairs for which the phase coherence is larger in the normal state than the preictal state.

Nearly all graphs show a preponderance of pairs of electrodes with higher phase coherence in normal subjects. The preponderance is strong in most frequency bands, and is particularly strong using C_z as a reference. Although there are quantitative differences among these three figures, each presents the same qualitative picture, i.e. that average phase coherence is larger in normal subjects than in epileptic patients, and that that difference is generally greater when comparing the interictal as opposed to the preictal state. This is true for the different cases and bands, and the choice of reference electrode does not materially affect the conclusions.

Preictal vs. Interictal states

We next examine the question of whether there is any difference in phase

coherence between the interictal state and preictal state by comparing the average phase coherence values of those two states directly. Refer to Fig. 2-3a and 2-3b. These figures are organized similar to Figs. 2-2. In each graph we plot the percentage of pairs for a given case and band for which the average phase coherence is statistically larger in the preictal state (blue), or interictal state (red). For most frequency bands and all cases, with the exception of the θ and α_2 band, Fig. 2-3a indicates a preponderance of pairs of electrodes with higher phase coherence associated with the preictal state than with the interictal state.

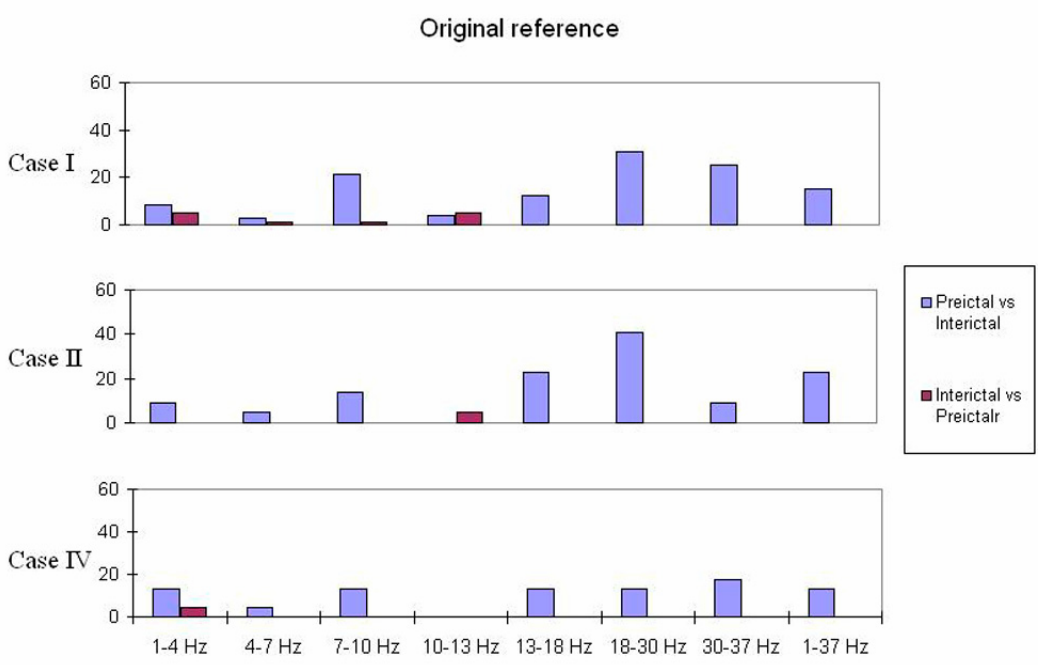

Figure 2-3a. Wilcoxon test results for phase coherence in preictal vs. interictal states using reference electrodes (P_1+P_2). Blue bars indicate the percentage of pairs for which the phase coherence is larger in the preictal state than the interictal state, and red bars indicate the percentage of pairs for which the phase coherence is larger in the interictal state than the preictal state.

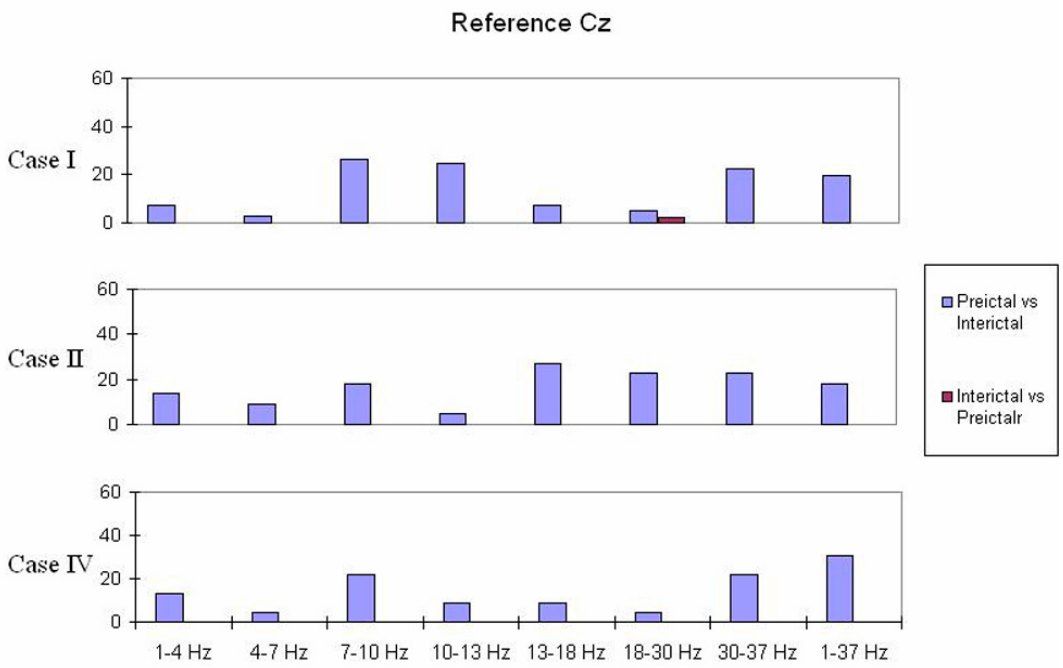

Figure 2-3b. Wilcoxon test results for phase coherence in preictal vs. interictal states using reference electrode C_z. Blue bars indicate the percentage of pairs for which the phase coherence is larger in the preictal state than the interictal state, and red bars indicate the percentage of pairs for which the phase coherence is larger in the interictal state than the preictal state.

2.6.1.2 Spatial Models without Controlling for Behavior States

For our regression analysis, the data was treated as follows: Each two hour epoch of data was filtered into eight bands, as described above. Each band filtered epoch was divided into 450 20-second windows with four second overlaps. A time counter was associated with each two hour segment. For a given case, state and reference electrode, the mean phase coherence over all pairs of electrodes was computed as a function of time for each two hour epoch. This time series of 450 values was further reduced by averaging successive 20-second windows in groups of 37 to produce a coarsened time series of 12 values associated with each two hour epoch.

Our regression model included a term for linear temporal dependence within an epoch, a term classifying the state (preictal, interictal or normal) and an interaction term multiplying time within an epoch by a variable classifying the state. We first checked for a statistically significant linear time dependence term within each epoch. We did not expect to see any significant temporal dependence in the interictal and normal data, and we did not. But we also did not see any significant temporal dependence in the preictal data. There may be several reasons for our failure to reject the null of no temporal dependence in the preictal data. However, the two most likely are the following: First, it could be that the preictal phase coherence does have a slope, but only closer to a seizure, so that two hours is too long a time over which to see a significant slope. (This would be consistent with our previous analyses of preictal data using marginal predictabilities (Li et al., 2003a). Second, it could be that the variance in the measurements of phase coherence is large enough to mask any statistical significance for the slope.

Having eliminated the temporal dependence we now ask whether our regression analysis indicates any dependence of phase coherence on state (interictal, preictal or normal). Specifically, we did three different regression analyses each of which compares two of the three states[2]. In this way we can test the null hypothesis that

[2] It is also possible to do these regression analyses using a single model. The results are qualitatively similar to those obtained using the approach outlined here. In particular, the p-values in Table Ia in the d band for cases I and II are lower (about 0.04 and 0.02, respectively).

there is no difference in average phase coherence between the two states[3]. To accommodate the serial correlations among phase coherence values from the same 2-hour epoch, we used a heterogeneous autoregressive covariance matrix in our linear mixed model. (We also performed the regression analysis using an unstructured covariance matrix and achieved similar results.) Finally, we repeated all our analyses for each of the three reference electrodes

Tables 2-1, 2-2 and 2-3 present the results for states (interictal vs. preictal, interictal vs. normal, and preictal vs. normal) respectively. Here we display p-values for rejection of the null hypothesis that the two states being compared have no difference in the mean phase coherence. Each table lists p-values for different cases and frequency bands. For clarity, values of $p<.05$ are displayed in bold.

[3] It is possible to question the validity of p-values due to multiple (three) comparisons among the three subgroups. This is a subject of on-going disagreement among statisticians. Here we adopt the point of view that asserts that when comparisons flow naturally from the plan of the experiment and which are not being used exploratorily to see what "might turn up", the usual type I error (p-value) is appropriate (Armitage and Berry, 1994). Since the comparisons between the normal state and the preictal state, and between the normal state and the interictal state serve the purpose of further illustrating the differences between the preictal and interictal state, we did not adopt correction techniques for the three comparisons.

Preictal vs. Interictal:

	δ	θ	α_1	α_2	β_1	β_2	γ	Broad
Case I	**0.0552**	0.0956	**0.0079**	0.4205	0.154	0.1085	0.5411	0.0823
Case II	**0.0534**	**0.0145**	**0.0025**	0.3356	0.088	0.1918	0.79	**0.0324**
Case III	0.1705	0.7642	0.1227	0.6962	0.91	0.4473	0.6709	0.8499
Case IV	0.2097	0.2781	**0.0189**	0.4278	0.1601	0.1681	0.5193	0.0586

(a) Original reference

	δ	θ	α_1	α_2	β_1	β_2	γ	Broad
Case I	**0.0529**	0.4208	0.0647	0.8494	0.3482	0.1629	**0.0274**	0.0894
Case II	**0.0416**	**0.0501**	**0.0312**	0.362	0.1771	0.3059	0.5203	0.059
Case III	**0.0461**	0.9063	**0.0515**	0.9683	0.6524	0.1699	**0.0497**	0.1685
Case IV	0.0667	0.4669	**0.0525**	0.8438	0.2947	0.1766	**0.0481**	0.2127

(b) Cz

Table 2-1. **P-values associated with the null hypothesis that average phase coherence (ρ) is the same in the interictal and preictal states, computed with different reference electrodes.** Rejection of the null ($p<0.05$) is shown in bold. For those cases of rejection, preictal phase coherence is larger than interictal phase coherence.

Interictal vs. Normal:

	δ	θ	α_1	α_2	β_1	β_2	γ	Broad
Case I	**<0.0001**	**0.0006**	**0.0003**	0.0578	**0.0008**	**0.0026**	**0.0348**	**<0.0001**
Case II	**<0.0001**	**<0.0001**	**<0.0001**	**0.0002**	**<0.0001**	**<0.0001**	**0.0037**	**<0.0001**
Case III	**<0.0001**	**0.0034**	**0.0022**	**0.0113**	**0.0017**	**0.0048**	**0.0068**	**0.0001**
Case IV	**0.0015**	**0.0082**	**0.0384**	0.2011	**0.0052**	**0.0115**	**0.0495**	**0.0014**

(a) Original reference

	δ	θ	α_1	α_2	β_1	β_2	γ	Broad
Case I	**<0.0001**	**0.0001**	**<0.0001**	**0.0003**	**<0.0001**	0.0734	**<0.0001**	**<0.0001**
Case II	**<0.0001**	**<0.0001**	**<0.0001**	**<0.0001**	**<0.0001**	**0.0016**	**<0.0001**	**<0.0001**
Case III	**<0.0001**	**<0.0001**	**<0.0001**	**<0.0001**	**<0.0001**	**0.0016**	**<0.0001**	**<0.0001**
Case IV	**<0.0001**	**0.0007**	**<0.0001**	**0.0005**	**<0.0001**	**0.047**	**<0.0001**	**<0.0001**

(b) Cz

Table 2-2. P-values associated with the null hypothesis that average phase coherence (ρ) is the same in the interictal and normal states, computed with different reference electrodes. Rejection of the null ($p<0.05$) is shown in bold. For those cases of rejection, normal phase coherence is larger than interictal phase coherence.

Preictal vs. Normal:

	δ	θ	α_1	α_2	β_1	β_2	γ	Broad
Case I	0.063	0.0956	**0.0079**	0.555	0.154	0.8273	0.2004	0.0823
Case II	0.0531	**0.0145**	**0.0025**	0.361	0.088	0.0791	**0.0232**	**0.0324**
Case III	**<0.0001**	0.7642	0.1227	0.204	0.91	**0.0522**	**0.0025**	0.8499
Case IV	0.1939	0.2781	**0.0189**	0.5702	0.1601	0.8692	0.2349	0.0586

(a) Original reference

	δ	θ	α_1	α_2	β_1	β_2	γ	Broad
Case I	0.0566	0.1257	**0.0199**	**0.0317**	0.3906	0.708	0.0638	0.0581
Case II	**0.0013**	0.0572	0.0606	**0.0045**	0.0893	0.1529	**0.0202**	**0.0315**
Case III	**<0.0001**	**<0.0001**	**<0.0001**	**0.0012**	**0.025**	0.0544	**0.0017**	**0.0002**
Case IV	0.1016	0.5171	**0.0386**	0.0635	0.4927	0.5772	**0.0382**	0.0662

(b) Cz

Table 2-3. P-values associated with the null hypothesis that average phase coherence (ρ) is the same in the preictal and normal states, computed with different reference electrodes. Rejection of the null ($p<0.05$) is shown in bold. For those cases of rejection, normal phase coherence is larger than preictal phase coherence.

Results of Regression Analysis

A cursory glance at these tables reveals the following high-level structures.

1. Table 2-1 (interictal vs. preictal) shows a rejection of the null in 7 to 10 of the cases (about 25-36%) for each of the two reference schemes. In the cases in which the null is rejected, preictal phase coherence is higher than interictal phase coherence.

2. Table 2-2 (interictal vs. normal) shows the most consistent rejection of the null across all frequency bands and cases, and for all reference electrodes. In the cases in which the null is rejected, normal phase coherence is higher than interictal phase coherence.

3. In table 2-3 (preictal vs. normal) the null is rejected in 25-47% of the cases depending on the choice of reference electrode. Choosing C_z as the reference

electrode give the best rejection of the null. In the cases in which the null is rejected, normal phase coherence is higher than pre-ictal phase coherence.

4. Generally, the choice of C_z as a reference electrode results in the strongest rejection of the null.

5. In table 2-1, the rejection of the null occurs most consistently in the α_1 band (and the γ band when C_z is the reference electrode).

6. In table 2-3, case III (phase coherence between a focal electrode and its homologous pair) shows the most consistent rejection of the null.

Many of these results are qualitatively consistent with those shown in Figures 2-2 and 2-3 using the Wilcoxon method. In particular, if we compare Table 2-2 and 2-3 with Figure 2-2, we see the same general picture of rejection of the null, which indicates statistically higher phase coherence values for the normal subjects. However, in the comparison between Table 2-1 and Figure 2-3, both of which compare the preictal vs. interictal states the situation is different. Here the Wilcoxon test shows a fairly consistent difference between phase coherence in these two states for most bands and cases, while Table 2-1 shows significance for only a few cases. The reason for this is that the within-group dispersion in measurements of interictal and preictal data used in the regression analysis is fairly large compared to the average separation between them. This obliterates the possibility of rejecting the null in many of the cases shown in Table 2-1. Furthermore, as we shall discuss in the next section, there are important spatial variations in the difference between interictal and preictal phase coherence. For some pairs of electrodes there is no

significant difference between preictal and interictal phase coherence, while for others there is a significant difference. This results in a diminution of sensitivity of a regression analysis by taking the average phase coherence across many pairs, e.g. 98 pairs in Case I. By contrast, the Wilcoxon rank-sum test is not as sensitive to the magnitude of the differences in the measurements, but only to which state has a higher value of the phase coherence. This effect is not as significant in Tables 2-2 and 2-3, which compare interictal and preictal to normal data, respectively, since the normal data has less dispersion.

2.6.2 Spatial Models with Controlling for Behavior States

In Tables 2-4 – 2-8 we present the p-values for rejecting the null hypotheses using data in which the average of electrodes P1 and P2 is used as a reference. We have also analyzed our data using Cz as a reference. These results will be discussed below, and the qualitative comparisons of these results with those obtained using (P1+P2) as a reference are shown in Tables 2-9 – 2-13. As is standard, we reject the null hypothesis (with 95% confidence) only if the associated p-value <0.05. In the previous section, without controlling for behavior state, we found a significant preictal increase only in the delta band. A brief analysis indicated that the overall increase in phase coherence preictally cannot be explained only by changes in behavior states. For all the models here, we perform a more detailed analysis and apply the linear mixed model with random intercept, to study the differences between interictal and preictal epochs for each behavior state, separately.

Model 1: mean phase coherence as a function of seizure state

First, we study the preictal change in phase coherence for all electrode pairs, controlling for behavior state. Our results (Table 2-4) show that the mean phase coherence values were significantly higher preictally for most bands during Awake, S1, S2 and REM sleep.[4] Differences in the γ band, on the other hand, were significant only for REM sleep. Clearly, differences in phase coherence between interictal and preictal states are also dependent on behavior state. More detailed spatial patterns of preictal increase in phase coherence are presented in the following models.

	Awake	Stage 1	Stage 2	Stage 3/4	REM
Delta	0.4321	0.0951	0.0661	0.2741	**0.0208**
Theta	**0.0081**	**0.0008**	**0.0003**	0.1548	**0.0133**
Alpha-2	**<.0001**	0.1645	**0.0009**	**0.0004**	**<.0001**
Beta-2	**0.0002**	**<.0001**	**<.0001**	0.0647	**<.0001**
Gamma	0.2656	0.9876	0.2242	0.8584	**0.0019**
Broad band	**0.0008**	**0.0074**	**0.0010**	0.2215	**0.0030**

Table 2-4. P values for rejecting the null hypothesis that there is no difference between preictal and interictal phase coherence averaged over all pairs.

Model 2: mean phase coherence as a function of electrode pair location (both members of the pair are either anterior or posterior) and seizure state (interictal or preictal).

In this model, there are variables that denote both the temporal proximity to a

[4] Note that, although no seizures occurred during REM sleep, portions of two-hour preictal epochs did coincide with REM sleep.

seizure as well as electrode pair location. The data used in this model are such that both electodes of a pair are either anterior or both are posterior. Estimate of the coefficient a_1 compares the average phase coherence between anterior and posterior pairs during interictal epochs. Our results indicated that the mean values of ρ for anterior pairs were significantly higher ($p<0.0001$) than for posterior pairs during interictal periods. Estimates of the coefficients b_1 and b_2 measure the changes in phase coherence between interictal and preictal epochs for the two groups (anterior and posterior) of electrode pairs respectively. For anterior pairs, we show, in Table 2-5a, p-values associated with rejection of the null hypothesis that there is no change in the average phase coherence (ρ) between interictal and preicatal epochs for various frequency bands and behavior states. All rejections of the null are due to increased phase coherence preictally. We see that for all behavior states, except for S3/S4 sleep, and for almost all frequency bands, there were significant preictal increases in phase coherence among anterior pairs. In Table 2-6a, we present the results of a similar analysis for posterior pairs. Here we see no significant changes in mean values of ρ during preictal periods compared to interictal periods. Thus, phase coherence values are generally higher in the anterior as opposed the posterior region of the brain, and, most importantly, *the phase coherence increases in the anterior region of the brain during preictal epochs, but does not increase in the posterior region preictally*.

It is worthwhile studying this strong preictal, anterior increase in phase coherence in more detail. To that end, we have divided our anterior electrode pairs

into two categories: interhemispherical (one member of a pair AI and the other AC) and intrahemispherical (both members of a pair AC or both AI). Roughly speaking, the former comprise primarily shorter range pairs, and the latter longer range pairs. In Tables 2-5b and 2-5c, we show, for different frequency bands and behavior states, the p-values associated with rejection of the null hypothesis that there is no change in the average ρ between interictal and preictal epochs. All rejections of the null are due to increased phase coherence preictally. We see a strong rejection of the null for many entries in both tables, although there is a stronger effect for the intrahemispherical electrode pairs in the anterior region. For completeness, we have also applied the same analysis to the posterior pairs, dividing them into intra-hemispherical and inter-hemispherical pairs. The results are shown in Tables 2-6b and 2-6c. We see no significant change in phase coherence between interictal and preicatal states in any of the groupings of posterior electrodes.

	Awake	Stage 1	Stage 2	Stage 3/4	REM
Delta	0.1158	0.3280	0.0678	0.9146	**0.0132**
Theta	**0.0259**	**0.0074**	**0.0003**	0.3003	**0.0038**
Alpha-2	**<.0001**	**0.0191**	**0.0001**	**0.0003**	**<.0001**
Beta-2	**0.0452**	**<.0001**	**<.0001**	0.2909	**0.0003**
Gamma	**0.0510**	0.9676	0.0038	0.9864	**0.0012**
Broad band	**0.0004**	**0.0073**	**0.0003**	0.4376	**0.0021**

Table 2-5a. P values for rejecting the null hypothesis that there is no difference between preictal and interictal phase coherence averaged over all anterior pairs.

	Awake	Stage 1	Stage 2	Stage 3/4	REM
Delta	0.3236	0.4909	0.4820	0.4412	**0.0481**
Theta	0.1334	0.2810	**0.0355**	0.8709	**0.0225**
Alpha-2	**0.0011**	0.2152	**0.0032**	**0.0089**	**<.0001**
Beta-2	0.2205	**0.0042**	**0.0026**	0.8072	**0.0231**
Gamma	**0.0149**	0.4807	0.1461	0.6248	0.0621
Broad band	**0.0050**	0.2896	**0.0310**	0.8371	**0.0212**

Table 2-5b. P values for rejecting the null hypothesis that there is no difference between preictal and interictal phase coherence averaged over all anterior long range pairs.

	Awake	Stage 1	Stage 2	Stage 3/4	REM
Delta	0.0841	**0.0180**	**0.0190**	0.3257	**0.0347**
Theta	**0.0223**	**0.0008**	**<.0001**	0.1198	**0.0174**
Alpha-2	**0.0002**	**0.0102**	**0.0004**	**0.0005**	**<.0001**
Beta-2	**0.0507**	**0.0002**	**<.0001**	0.1127	**0.0002**
Gamma	0.4149	0.5172	**0.0019**	0.6539	**0.0008**
Broad band	**0.0022**	**0.0009**	**0.0001**	0.1328	**0.0061**

Table 2-5c. P values for rejecting the null hypothesis that there is no difference between preictal and interictal phase coherence averaged over all anterior local pairs.

	Awake	Stage 1	Stage 2	Stage 3/4	REM
Delta	0.7053	0.9200	0.9229	0.4213	0.4113
Theta	0.7289	0.6741	0.7391	0.3523	0.5112
Alpha-2	0.6822	0.7952	0.7031	0.3140	0.1817
Beta-2	0.2045	0.2938	0.6163	0.2084	0.1631
Gamma	0.7119	0.6003	0.2588	0.5748	0.4963
Broad band	0.6510	0.7950	0.6229	0.4258	0.2960

Table 2-6a. P values for rejecting the null hypothesis that there is no difference between preictal and interictal phase coherence averaged over all posterior pairs.

	Awake	Stage 1	Stage 2	Stage 3/4	REM
Delta	0.5467	0.8204	0.7266	0.5526	0.5929
Theta	0.9645	0.7187	0.6786	0.6655	0.9219
Alpha-2	0.8175	0.6592	0.9426	0.4947	0.7118
Beta-2	0.3159	0.4819	0.7390	0.1836	0.5872
Gamma	0.9116	0.6985	0.4220	0.3138	0.9184
Broad band	0.8303	0.8515	0.9434	0.6727	0.6814

Table 2-6b. P values for rejecting the null hypothesis that there is no difference between preictal and interictal phase coherence averaged over all posterior long range pairs.

	Awake	Stage 1	Stage 2	Stage 3/4	REM
Delta	0.9931	0.6656	0.8257	0.4713	0.3962
Theta	0.4893	0.2626	0.2996	0.2527	0.2067
Alpha-2	0.6605	0.9756	0.4607	0.3035	0.0516
Beta-2	0.2849	0.3052	0.6125	0.3908	0.0691
Gamma	0.6425	0.6461	0.3099	0.9093	0.2961
Broad band	0.5724	0.5203	0.4376	0.3608	0.1696

Table 2-6c. P values for rejecting the null hypothesis that there is no difference between preictal and interictal phase coherence averaged over all posterior local pairs.

Model 3: mean phase coherence as a function of electrode pair location (one member of the pair is anterior and the other is posterior, but both are either ipsilateral or contralateral) and seizure state

Another linear mixed model was used to study phase coherence of electrode pairs that connect the anterior and posterior halves of the brain such that both electrodes come from the same hemisphere. There are two classes of such pairs: A. Those pairs in which both electrodes are on the side of the brain ipsilateral to the seizure focus and B. Those pairs in which both electrodes are on the side of the brain

contralateral to the seizure focus.

In Tables 2-7a and 2-7b, we present results on the difference between preictal and interictal mean phase coherence for these two classes of electrodes. In general, about 30% of the entries in these tables show significant preictal increases in phase coherence in both the ipsilateral and contralateral hemispheres. The β_2 band seemed to have the most consistent preictal increase in phase coherence across different behavior states in both hemispheres. In addition, α_2 and β_2 had significant increases in preictal phase coherence during REM sleep in both hemispheres. In addition, ipsilateral pairs showed consistent increases in preictal phase coherence across several bands in stage one and stage two sleep.

	Awake	Stage 1	Stage 2	Stage 3/4	REM
Delta	0.8208	**0.0327**	**0.0385**	0.1260	0.6822
Theta	0.2761	**0.0164**	**0.0079**	0.2794	0.4875
Alpha-2	0.2288	0.5330	0.1300	0.3229	**0.0214**
Beta-2	**0.0172**	**0.0011**	**0.0013**	0.3096	**0.0333**
Gamma	0.6399	0.2587	0.4475	0.9547	0.1350
Broad band	0.3001	0.1067	0.0641	0.2582	0.3850

Table 2-7a. P values for rejecting the null hypothesis that there is no difference between preictal and interictal phase coherence for ipsilateral A-P pairs

	Awake	Stage 1	Stage 2	Stage 3/4	REM
Delta	0.2638	0.0727	0.4408	0.5065	0.5463
Theta	**0.0112**	**0.0148**	0.1425	0.5918	0.4543
Alpha-2	0.0661	0.8039	0.2309	0.1588	**0.0019**
Beta-2	**0.0041**	**0.0236**	**0.0342**	0.3002	**0.0120**
Gamma	0.1946	0.9207	0.7112	0.8797	0.0815
Broad band	**0.0305**	0.1144	0.3767	0.6956	0.2498

Table 2-7b. P values for rejecting the null hypothesis that there is no difference between preictal and interictal phase coherence for contralateral A-P pairs

Model 4: mean phase coherence as a function of electrode pair location (pair members in opposite hemispheres anterior-posterior as well as ipsilateral-contralateral) and seizure state

In this model we studied the phase coherence of electrode pairs such that the two members of the pair lie in opposite hemispheres of the brain, both anterior-posterior and ipsilateral-contralateral. These pairs can be put into one of two categories: A. Pairs consisting of AI and PC and B. Pairs consisting of AC and PI. The results of this model are presented in Tables 2-8a and 2-8b for various frequency bands and behavior states. There are several cases in which the null is rejected. As before, all rejections are due to an increase in preictal phase coherence. It is noteworthy that the strongest rejections of the null occur in the β_2 band during wakefulness and stage one sleep. There is also significance in this table in the δ band during wakefulness, but, as we shall see, this result is not robust to a change reference electrode.

	Awake	Stage 1	Stage 2	Stage 3/4	REM
Delta	**<.0001**	0.5611	0.4077	0.5733	0.3125
Theta	**0.0301**	0.1403	0.2887	0.8546	0.9456
Alpha-2	0.2600	0.1687	0.6106	0.1180	0.0644
Beta-2	**<.0001**	**0.0045**	0.2444	0.4577	0.9260
Gamma	0.5081	0.2641	0.0083	0.5625	0.8102
Broad band	0.0948	0.6690	0.6565	0.8483	0.4063

Table 2-8a. P values for rejecting the null hypothesis that there is no difference between preictal and interictal phase coherence for Ipsilateral Anterior-Contralateral Posterior pairs

	Awake	Stage 1	Stage 2	Stage 3/4	REM
Delta	**<.0001**	0.2444	0.3809	**0.0466**	0.2243
Theta	0.2599	**0.0158**	0.0524	0.3904	0.3794
Alpha-2	0.1292	0.6534	0.4032	0.2326	**0.0003**
Beta-2	**<.0001**	**<.0001**	0.0002	0.1020	**0.0032**
Gamma	0.8114	0.8102	0.8874	0.4905	0.1105
Broad band	0.3588	0.1848	0.1277	0.2136	0.1612

Table 2-8b. P values for rejecting the null hypothesis that there is no difference between preictal and interictal phase coherence for Contralateral Anterior-Ipsilateral Posterior pairs

Comparisons with results using Cz as the reference electrode.

We have repeated these analyses using Cz as the reference electrode. Rather than presenting tables of p-values for these analyses, we present, in Tables 2-9 - 2-13 a graphic representation that indicates which preictal increase in phase coherence are robust to changes of the reference electrode and which are not. These tables mirror Tables 2-4 – 2-8 (i.e., Table 2-9 refers to the same data as Table 2-4, Table 2-10 refers to the same data as Table 2-5, etc.). Boxes colored black are those combinations of frequency band and behavior state for which there are statistically significant increases in preictal phase coherence with both (P1+P2) and Cz as the reference signal. Boxes colored gray have a statistically significant increase in preictal phase coherence for one, but not both of the reference schemes, and boxes that are white do not have a significant preictal increase in phase coherence for either reference scheme. Note also, that nearly all the gray boxes are due to statistical significance when using Cz as the reference electrode. Note, also, that because they are not particularly informative, we have not included broad-band results in Tables 2-9 – 2-13.

	Awake	Stage 1	Stage 2	Stage 3/4	REM
Delta					
Theta					
Alpha-2					
Beta-2					
Gamma					

Table 2-9. Preictal change for all pairs (see also Table 2-4). Black: statistically significant increase in preictal phase coherence with both (P1+P2) and Cz as the reference signal; Gray: statistically significant increase in preictal phase coherence for one, but not both of the reference schemes; White: no significant preictal increase in phase coherence for either reference scheme.

	Awake	Stage 1	Stage 2	Stage 3/4	REM
Delta					
Theta					
Alpha-2					
Beta-2					
Gamma					

Table 2-10a. Preictal change of all anterior pairs (see also Table 2-5a). Color scheme as in Table 2-9.

	Awake	Stage 1	Stage 2	Stage 3/4	REM
Delta					
Theta					
Alpha-2					
Beta-2					
Gamma					

Table 2-10b. Preictal change of anterior long range pairs (see also Table 2-5b). Color scheme as in Table 2-9.

	Awake	Stage 1	Stage 2	Stage 3/4	REM
Delta					
Theta					
Alpha-2					
Beta-2					
Gamma					

Table 2-10c. Preictal change of anterior local pairs (see also Table 2-5c). Color scheme as in Table 2-9.

	Awake	Stage 1	Stage 2	Stage 3/4	REM
Delta					
Theta					
Alpha-2					
Beta-2					
Gamma					

Table 2-11a. Preictal change of all posterior pairs (see also Table 2-6a). Color scheme as in Table 2-9.

	Awake	Stage 1	Stage 2	Stage 3/4	REM
Delta					
Theta					
Alpha-2					
Beta-2					
Gamma					

Table 2-11b. Preictal change of posterior long range pairs (see also Table 2-6b). Color scheme as in Table 2-9.

	Awake	Stage 1	Stage 2	Stage 3/4	REM
Delta					
Theta					
Alpha-2					
Beta-2					
Gamma					

Table 2-11c. Preictal change of posterior local pairs (see also Table 2-6c). Color scheme as in Table 2-9.

	Awake	Stage 1	Stage 2	Stage 3/4	REM
Delta					
Theta					
Alpha-2					
Beta-2					
Gamma					

Table 2-12a. Preictal change of ipsilateral A-P pairs (see also Table 2-7a). Color scheme as in Table 2-9.

	Awake	Stage 1	Stage 2	Stage 3/4	REM
Delta					
Theta					
Alpha-2					
Beta-2					
Gamma					

Table 2-12b. Preictal change of contralateral A-P pairs (see also Table 2-7b). Color scheme as in Table 2-9.

	Awake	Stage 1	Stage 2	Stage 3/4	REM
Delta					
Theta					
Alpha-2					
Beta-2					
Gamma					

Table 2-13a. Preictal change of Ipsilateral Anterior-Contralateral Posterior pairs (see also Table 2-8a). Color scheme as in Table 2-9.

	Awake	Stage 1	Stage 2	Stage 3/4	REM
Delta					
Theta					
Alpha-2					
Beta-2					
Gamma					

Table 2-13b. Preictal change of Contralateral Anterior-Ipsilateral Posterior pairs (see also Table 2-8b). Color scheme as in Table 2-9.

2.7 Discussions

2.7.1 Wilcoxon Rank-Sum Test and Spatial Models Without Controlling for Behavior States

We implemented the spatial models for two objectives. The first is to study the general dependence of phase coherence between EEG scalp electrodes as a function of time to seizure in patients with temporal lobe epilepsy, and also to compare that phase coherence with similar measurements on normal subjects. The second is to examine the dependence of these measures on realistic choices of reference electrodes. The effects of behavior states were not considered because a small sample of balanced

behavior states was selected.

It is important to first discuss the dependence of these phase coherence measures on reference electrodes, since, if there were no consistency among those, we would not be able to make any meaningful statements, even qualitative empirical ones. Fortunately, there is significant consistency among our measurements. While we have shown that (not surprisingly) there are quantitative differences in both the Wilcoxon results and the regression results among calculations with different choices of reference electrodes, the general picture that emerges is qualitatively independent of the choice of reference electrode. In all cases we find, using the Wilcoxon metrics, that interictal phase coherence is generally smaller than preictal phase coherence, and that interictal phase coherences are smaller than corresponding quantities in normal subjects. Preictal phase coherences are closer to those of normal subjects, but in some cases (notably the θ and α_2 band when using P_1+P_2 as the reference electrode) are somewhat smaller. Interestingly, choosing C_z as the reference electrode does seem to increase the sensitivity to differences in phase coherence between the normal state and the interictal and preictal states. Part of this increased sensitivity, particularly in the higher frequency bands, may be due to the significant power in these bands known to be generated in the regions of the P electrodes$_z$. Large power associated with one electrode (in this case, the reference electrode) in a given frequency band, will tend to dominate the phase structure of the resulting voltage difference time series. If the same reference electrode is used for two series, then we expect that differences in the phase structure between those two

series will be small. This is consistent with our results. (See, for example, results in Figs. 2-2b) We are uncertain about whether this is the whole answer to C_z's increased sensitivity although from a strictly empirical perspective it doesn't matter: It appears that using C_z as a reference electrode is a good choice if one is interested in distinguishing empirically between normal subjects and epileptic patients. This does, however, leave an interesting question unanswered. Similarly, the regression results are qualitatively the same using different reference electrodes, although there are quantitative differences that lead to different p-values and to some variation in statistical significance in results using different reference electrodes.

Despite the qualitative utility of phase coherence measurements, it would be very useful (particularly for the studies suggested below) to have a nonlinear measure that is very sensitive to information transfer but that does not depend on the choice of reference electrode. There are a number of candidates, including application of marginal predictabilities (MP) (Savit and Green, 1991) to the phase of the difference between two electrodes. Computing the difference of two electrodes removes the reference signal. For a wide class of functional couplings, if the phase of the difference of the two electrodes is I.I.D., then we can suppose that the signals are uncoupled. MP is very sensitive to deviations from I.I.D. and so may be a sensitive indicator of absence of information transfer between these electrodes, in this sense. Rejection of the null of I.I.D. implies non-zero values of MP. But non-zero values of various orders of MP also carry dynamical information about the structure of the (non-I.I.D.) time series, and so may provide hints about the nature of the information

transfer between the electrodes. This will be further discussed elsewhere.

The fact that the phase coherence measurements using different reference electrodes are qualitatively similar, but quantitatively different, suggests that the most meaningful statements will be those that refer to the general structure common to all the reference electrodes, and that one should be circumspect about drawing firm conclusions about the details. This will guide our comments in the rest of this section, as we turn to a discussion of the dependence of phase coherence on state (interictal, preictal, normal).

The most obvious, and most important conclusion from this study is that interictal phase coherence is lower than either preictal phase coherence or phase coherence in normal subjects. This is most clear using the Wilcoxon test and is qualitatively independent of the choice of reference electrode. As a qualitative statement, this is also independent of frequency band, except when comparing interictal to preictal states in the γ band. Here there is a much less pronounced difference in phase coherence indicated in the Wilcoxon graphs, but there is significance in some cases using the regression analysis.

When we compare preictal to normal states, we find, generally, a less marked difference in phase coherence. Indeed, the Wilcoxon graphs show no real difference in phase coherence unless C_z is used as a reference. Similarly, the regression analysis shows little difference between the phase coherence in these two states *except* in case III, in which we compare two homologus electrodes, one near the seizure focus and one contralateral to it. Here we see a consistent difference in phase

coherence in most frequency bands.

What are we to make of these observations? Consistent with our epistemology, we abstain from commenting on the detailed results. But the general pattern that emerges is suggestive. If the phase coherence between two electrodes is high, we expect that the regions of the brain associated with those electrodes will share information, either by direct or indirect communication. Low phase coherence, on the other hand suggests a lack of information transfer between those regions of the brain. (This latter statement, though, needs to be taken with a grain of salt. Even though phase coherence is low, it is possible that information is shared, but leads to more subtle correlations in neural activity.) The general pattern of lower phase coherence interictally suggests a diminution in the epileptic brain's ability to communicate information across macroscopic distances. The larger value of phase coherence preictally suggests an increase in communication among distant parts of the brain preceding a seizure. This is also consistent with the picture suggested by our previous work using marginal predictabilities (Li et al., 2003a, 2003b, 2006). There we found that the differences in marginal predictabilities were smaller several tens of minutes prior to a seizure that they were interictally, again suggesting increased ease of communication among widely separated parts of the brain sometime prior to a seizure. Both these studies imply increased macroscopic communication well before any clinical or electrographic signs of a seizure. The qualitative large scale dynamics implied by these observations is that large scale seizures are inhibited (interictally) by a decreased ability of the epileptic brain to communicate well over

long distances. This is consistent with the observation that interictal phase coherence is smaller than that seen in normal subjects. Sometimes, however, the ability of the epileptic brain to communicate well increases. This sets the stage for the pathological paroxysmal neural activity that occurs near the seizure focus to spread to distant parts of the brain, resulting in a full-blown seizure. Similar questions concerning short- and long-range coherences have also been studied in other CNS diseases (Stam et al., 2006; Cover et al., 2006).

This qualitative picture is appealing and raises a number of questions. First, it is unclear whether the epileptic brain has reduced information transfer interictally across the whole brain, or whether there is only functional isolation of the seizure focus. Either option is consistent with our observations. The answer to this question may have implications for the behavior of ictogenesis in nonfocal epilepsies, compared to focal epilepsies. Studies of nonlinear correlative metrics in patients with nonfocal epilepsies would be most informative here. Second, a better understanding of reduced information transfer in the epileptic brain may help illuminate the origin of cognitive deficits often associated with epilepsy. The fact that people with epilepsy spend much of their lives in a state in which it is relatively difficult to transfer information among different parts of the brain may be of significance in the development of cognitive deficits. Studies correlating spatial patterns of reduced interictal information transfer with specific patterns of cognitive deficits should help assess this possibility. Third, it would also be interesting to correlate reduced interictal information transfer with anti-epileptic therapies,

including drug regimes and stimulation protocols. It would be most interesting to know what effect different therapies have on the brain's ability to communicate over large distances.

A fourth interesting set of questions concerns comparisons of our results with several papers which report nonlinear analyses of data from intracranial electrodes. As we begin this discussion it is important to bear in mind that the data used in the intracranial studies is of a very different nature than our scalp data. The intracranial data are much less noisy and of much shorter duration, the electrodes record from much smaller brain regions, and typically analyses that compare more than one electrode extend over limited regions of the brain, often limited to the neighborhood of the seizure focus. Furthermore, different definitions of "preictal" are sometimes used, often referring to epochs of no more than a few minutes prior to seizure onset. Nevertheless it is useful to comment on these analyses.

In a study of phase coherence from intracranial electrodes, Mormann, et al., (2003) showed that in focal epilepsy, phase coherence over short distances near the seizure focus (and sometimes contralateral to the seizure focus) *decreased* prior to a seizure. (Related work by Le Van Quyen et al., (2005) shows a somewhat more complex preictal phase coherence structure (sometimes increasing, sometimes decreasing), but again, from intracranial, relatively short distance measurements.) A simple model (Feldt et al., 2007) suggests that the decrease observed by Mormann, et al., (2003) sets the stage for the paroxysmal neural activity at the seizure focus to entrain nearby regions, thus allowing local propagation of the seizure. At first sight,

this work appears to be in contradiction to our own. There are, of course, many methodological differences between the study of Mormann et al., (2003) and ours. Mormann et al., (2003) study broad-band phase coherence, they are looking at phenomena over a much shorter length scale, and the nature of the data set they use (recording from intracranial electrodes) is much different than the scalp data we use. (Many of these same methodological considerations apply also to the work of Le Van Quyen et al., 2005.) Nevertheless, it would be useful if qualitative comparisons could be made. How then, do we reconcile the preictal decrease in phase coherence reported by Mormann et al., (2003) and our observation of a preictal *increase*? The suggestion in Mormann et al., (2003) is that the decrease in phase coherence is often associated with regions of the brain close to seizure focus, and which then become recruited into the spreading paroxysmal activity of the seizure. In this picture, the decrease in synchronization might be thought of as preceding a local wave front that propagates with the spreading seizure, at least in its initial stages. By contrast, the preictal increase in phase coherence that we observe is a much longer-range phenomenon and its spatial variations are quite different (Zhang et al., 2009a). The two phenomena are not contradictory, but what the precise dynamical relation between is remains unclear. Similarly, there is no contradiction in a comparison of our work to the more complicated short range, interictal picture suggested by Le Van Quyen et al., (2005). We also note that Schevon et al., (2007) using interictal intracranial EEG observe patient specific patterns of interictal hypersynchonization in the focal region of patients with partial epilepsy. In addition, Blumenfeld et al.,

(2007) report increased *linear* correlation between the frontal region and the amygdala in amygdala kindled rats, both ictally and interictally which they associate with stronger frontal-amygdala signaling. Bettus et al., (2008) found higher interictal nonlinear correlation in interictal, intracranial EEG data taken from the temporal lobe in patients with MTLE, for whom the temporal lobe was the focal region than for patients with focal epilepsy, but whose focal region was not in the temporal lobe. This suggests a stronger functional connectivity in the focal region, but says nothing about information transfer across much larger regions. Again, because of the different nature of the data (intracranial, largely short-distance as opposed to scalp, long-distance) and the different methods of analysis (linear, for example, in the case of Blumenfeld et al., 2007), it is difficult to draw simple dynamical conclusions. A careful study of simultaneously recorded scalp and intracranial data would be very helpful in addressing these kinds of questions.

A few other studies that analyze intracranial recordings and concern themselves with either ictal events or times very close to seizure onset in TLE are also worth mentioning. Schindler et al., (2007) observed no change or decreases in the correlation of EEG channels during the first half of a seizure, and increases in the second half. Similarly, Guye et al., (2008) using intracranial recordings reported that values of non-linear correlation between the thalamus and temporal lobe structures at the beginning of a seizure were significantly higher than values from the "background" period (at least one minute prior to the onset of ictal discharge), while values at the end of the seizure were higher than those at seizure onset. In another

study, Bartolomei et al., (2004) found significant increases in nonlinear correlation coefficients among mesial structures just prior (seconds) to rapid ictal discharge. These studies taken together paint an intricate and complex picture of the nature of correlations in electrical activity in brain regions near the seizure focus and for times close to ictal onset. We emphasize that they are not in contradiction with our findings since our work is based on much longer temporal and spatial scales using a very different sort of data set: Our results should be understood as representing a general long-term trend in electrical activity among widely separated brain regions as an epileptic seizure is approached, rather than referring to more localized observations within seconds of seizure onset.

In this part we have shown that, generally, interictal phase coherence measured from pairs of scalp electrodes in subjects with temporal lobe epilepsy is significant lower than corresponding measurements in normal subjects. We have also shown that during preictal epochs (within two hours prior to a seizure) phase coherence levels rise to levels approaching those found in normal subjects. These general trends obtain even after controlling for behavior state. It is unclear whether this phenomenon is consistent and robust enough to be of use in designing non-invasive seizure prediction devices. But even if they do not have proximate practical application, our observations are, as we have discussed, suggestive of an intriguing general dynamic that may be important in seizure propagation.

2.7.2 Spatial Models Controlling for Behavior States

The primary purpose of these models is to examine the anatomical pattern of phase coherence measures derived from scalp EEG, particularly comparing interictal and preictal periods in subjects with temporal lobe epilepsy. We have performed these analyses for a variety of different frequency bands and behavior states, and for two different reference schemes. We have given strongest credence to those results that are robust to changes in the reference electrode scheme.

Our main findings are easiest to summarize if we adopt the following notation: Let $\Delta\rho(X,Y)$ stand for the differences in average phase coherence (preictal phase coherence minus interictal phase coherence) between pairs of electrodes, one of which is in region X of the brain and the other in region Y, where X and Y are one of AI, AC, PI or PC. Our main findings are the following:

1. $\Delta\rho(X,Y)$ is significantly positive when X and Y are both anterior regions of the brain.
2. $\Delta\rho(X,Y)$ is, generally, not significantly different from zero when X and Y are both posterior regions of the brain.
3. If X=AI and Y=PI, $\Delta\rho(X,Y)$ is significantly positive for about one-third the cases of behavior state and frequency band.
4. If X=AC and Y=PC, $\Delta\rho(X,Y)$ is significantly positive for about one-third the cases of behavior state and frequency band.
5. The combinations of behavior states and frequency bands for which there is significance of $\Delta\rho(X,Y)$ in 3 and 4 are not identical. However, the β_2 band does seem to show robustness between ipsilateral and

contralateral cases.

6. For (X,Y)=(AI,PC) or (AC,PI), $\Delta\rho(X,Y)$ is not significantly different from zero for most cases of (behavior state, frequency band). Among the few significant results, we find significance in the β_2 band in the awake and stage one sleep states (X,Y)=(AI,PC) and (AC,PI) independent of electrode reference scheme.

7. Of all frequency bands, the β_2 band is most strongly associated with a preictal increase in phase coherence across different sets of electrode pairs and behavior states.

8. Relative to other behavior states, there is almost never an increase in preictal phase coherence during stage 3/4 sleep.

We will first discuss these findings. Then we will summarize and discuss other, more detailed aspects of our results, in particular, more detailed structure differences of preictal and interictal phase coherence as a function of frequency and behavior state.

The results described above show that, phase coherence increases preictally among anterior pairs of electrodes, while there is no general increase in phase coherence among pairs of posterior electrodes. These results are consistent with our findings in the previous section, in which we showed that there was a general increase in phase coherence of scalp electrodes, preictally, in patients with TLE. Our results here are also consistent with the common clinical observation that seizures in TLE spread primarily through the anterior regions of the brain. For example, Blume et al.,

(2001) have shown that seizures which originate in the temporal lobe direct more commonly first to the contiguous frontal cortex than to the opposite hemisphere. Our observations of an anterior increase in phase coherence preictally (defined as up to two hours prior to a seizure) provides further support for the picture we have suggested elsewhere (Drury et al., 2003; Li et al., 2003a, 2003b, 2006; Zhang et al., 2009a) concerning the role of information channels in seizure propagation. Recall that we have observed that various bilocal, nonlinear metrics (marginal predictability and phase coherence) indicate that information transfer across large distances is reduced interictally in patients with TLE, compared to normals. In addition, these same metrics show that information transfer generally increases preictally, well before any clinical or standard electrographic signs of a seizure. These observations suggest that in the epileptic brain information transfer is suppressed over long distances, interictally, and this suppression contributes to the functional isolation of the seizure focus. While the focus is functionally isolated, it is difficult to entrain distant regions of the brain, and thus to develop a full-blown seizure. However, sometimes long-distance communication channels in the brain reopen and this functional isolation breaks down, setting the stage for the paroxysmal neural activity associated with the seizure focus to propagate to distant parts of the brain, and thus, for the development of a seizure. In support of this picture, we have shown that preictal increases in phase coherence occur preferentially in anterior regions of the brain up to two hours prior to seizure onset, which is the route through which seizures in TLE are observed to propagate. It is also worthwhile adding here that we

understand an increase in "information transfer" in a broad sense, roughly representative of increased functional connectivity between given regions of the brain. This picture of decreased interictal communication in the epileptic brain, with a subsequent preictal increase is also supported by our results on the β_2 band. We have found that a preictal increase in phase coherence in the β_2 band is fairly robust across many spatial and behavior state configurations. Kopell et al., (2000) have argued that the β band is employed in long distance communication in the brain. This suggestion is consistent with our notion that enhanced long-distance communication in the brain, as indicated by increased phase coherence, precedes seizure formation.

Another striking result of our analysis, is the near absence of any preictal increase in phase coherence during stage 3/4 sleep. While there may be a dynamical explanation for this observation, the most likely one appears to be the fact that this stage of deep sleep is, in any case, marked by high EEG synchrony. This high degree of background synchrony may make it difficult to observe additional increases in phase coherence during preictal periods.[5]

In addition to these general patterns, the Tables also contain a number of other more detailed systematic results. First, from Tables 2-10b and 2-10c (see also Tables 2-5b and 2-5c), we note that $\Delta\rho(X,Y)$ for anterior pairs is more likely to be significantly positive when both electrodes are either ipsilateral or contralateral (Table 2-10b) to the seizure focus. Anterior pairs that connect the ipsilateral to the

[5] We thank Jack Parent for helpful discussions on this point.

contralateral side of the brain (Table 7c), do often have values of $\Delta\rho(X,Y)$ that are positive, but the effect is more robust across different frequency bands and behavior states for intrahemispherical anterior pairs.

Another interesting result is contained in Tables 2-12a and 2-12b (see also Tables 2-7a and 2-7b). Here we see that $\Delta\rho(X,Y)$ between AP pairs has somewhat more significant entries on the ipsilateral than on the contralateral side. Of note is the fact that, with the exception of S3/S4 sleep, the β_2 band is always significant in both tables. $\Delta\rho(X,Y)$ is significant also on the ipsilateral side in stage 1 and stage 2 sleep for low frequencies and is significant during REM sleep in the α_2 and β_2 bands.

We also note, in Tables 2-13a and 2-13b (see also Tables 2-8a and 2-8b) that $\Delta\rho(X,Y)$ is significantly positive in the β_2 band in the awake and stage 1 states for (X,Y)=(AI,PC) and (AC,PI). This again points to the robustness and likely importance of the β band for long distance communication in the brain. The other apparently robust increases in these tables, namely, increases in θ in the awake state (Table 2-13a) and increases in δ in stage 3/4 and in β_2 in REM (Table 2-13b) may be significant, but, in our view, would benefit from additional corroborating data, or additional biological arguments.

Although these, and other detailed results are intriguing, it is unclear to what extent they are generic and to what extent they reflect idiosyncrasies of the particular population used in this study. Although we were at pains to define as homogeneous a cohort of subjects as possible, there is still great variation in both electrographic and clinical manifestations of temporal lobe seizures from one subject to the next. It

seems quite likely that our most general conclusions—the larger difference in the behavior of anterior and posterior phase coherence preictally and the importance of the β band—are robust. But it may be that some of the details of the tables could depend on the particular subject population.

A corollary to this is that patterns of phase coherence in subjects with epilepsy may be associated with specific cognitive deficits. It is well known that certain cognitive deficits are common in subjects with TLE, but there is significant variation of the extent to which these deficits are present. It is known, for instance, (Helmstaedte et al., 2004) that left hemisphere foci often result in verbal learning deficits and right hemisphere foci preferentially in figural learning deficits. Moreover, deficits in memory may also be heterogeneous. Particularly for those deficits that involve extended regions of the brain, it is not unreasonable to suppose that the deficits are not due only to focal, temporal lobe anomalies, but are a consequence of the inhibited interical ability of the epileptic brain to communicate and transfer information over long distances. Given the heterogeneity of cognitive deficits, it would not be surprising to find heterogeneity in the details of phase coherence across the brain, also. A more complete discussion of the relationship between patterns of phase coherence and cognitive deficits in subjects with epilepsy will be presented elsewhere.

Another question that naturally arises is whether these metrics, or related ones, which are associated with preictal changes can be used as the basis for a reliable seizure prediction method. Although there are certainly reasons to pursue this

approach, there are many obstacles to overcome. The most difficult may be the intrinsic heterogeneity from subject to subject and even from seizure to seizure. The results presented here are population results averaged over a number of patients and seizures. The robustness of these metrics applied to individual seizures may be a very different story.

In this study, we have focused on subjects with TLE. But if the idea of enhanced long distance communication as a precursor to ictogenesis is correct, one might expect to see similar results associated with other types of epilepsy. Similar studies on subjects with other types of focal and generalized epilepsies could be most informative, and could help elucidate the nature of ictogenesis and role of long-distance preictal communication in the brain.

2.8 Summary

Compared to normal subjects, we have found that phase coherence is reduced for epileptics during interictal periods (defined as at least two hours away from any seizure) but increased during preictal periods (within two hours prior to a seizure). This suggests a lack of information transfer of the brain in epilepsy patients during interictal periods, but not, during preictal periods. We surmise that the increased communication that seems to presage a seizure is responsible for allowing the seizure to spread from its focal origin to distant parts of the brain. Furthermore, the geographical pattern of preictal changes in phase coherence is of interest. Our results indicated increased phase coherence in the anterior region compared to the

posterior region in the preictal period. Our study has carefully examined this proposed mechanism of seizure spread, and its anatomical distribution by studying the large-scale behavior of phase coherence (and related nonlinear metrics) in detail.

Contrary to popular belief, sleep is not a static process, but a series of complex stages of synchronous brain waves. A study of 264 sleep seizures has reported that sleep seizures begin during stages one (23%) and two (68%) but are rare in slow-wave sleep; no seizures occurred during rapid eye movement (REM) sleep. In our study, the impact of behavior state was examined between interictal and preictal epochs within each frequency band. We observed increased phase coherence during sleep stage one and two, and reduced phase coherence in slow wave sleep and REM sleep. The second question examined is the geographical pattern of preictal change in phase coherence. Consistent with the belief that TLE seizures mainly propagate in the anterior region of the brain, we found increased phase coherence in the anterior region compared to the posterior region.

For this study, scalp EEG data of TLE patients were obtained from the Henry Ford Hospital. An epileptologist validated the times of seizure onset, as well as the behavior state of the subject. The EEG data were filtered to five frequency bands of major clinical interest and categorized by behavior state and seizure state (interictal and preictal). A battery of statistical techniques was used to correlate the changes in long-distance phase coherence and other non-linear metrics with frequency, behavior state, epileptic state (preictal or interictal), and anatomical position on the scalp. A number of other technical issues were addressed, including the dependence of

measurements on the choice of reference electrode.

This work is directed to two outcomes. First, our detailed study of phase coherence will improve our understanding of seizure generation and propagation. Second, and very importantly, our studies may lay the groundwork for the development of a non-invasive, reliable method of seizure prediction. If one is able to predict seizures reliably, one may be able to develop acute therapies that can be used to abort the seizures. This will be a major step forward in the treatment of epilepsy, particularly for those patients whose conditions are medically intractable.

CHAPTER 3

PHOTIC-DRIVEN NONLINEAR DYNAMICS AND A SCALP EEG BIOMARKER FOR ALZHEIMER'S DISEASE

3.1 Introduction

Clinical features of Alzheimer's disease (AD) include dysfunction in memory and cognition, with underlying pathological changes including extracelluar deposition of beta amyloid protein to form plaques, and intracellular aggregation of phosphorylated tau protein, giving rise to neurofibrillary tangles. Although there are many clinical and biological concomitants to AD, there is, as yet, no unequivocal and practical biomarker for AD. There is also little in the way of understanding of the long distance brain dynamics associated with AD, even though long distance functional integration is crucial for cognitive functioning (Fuster JM et al., 2003). Analyses of EEG data may be useful in addressing both these issues. EEG is an inexpensive, non-invasive procedure and contains considerable information about the long distance behavior of the brain.

A number of EEG studies have been carried out on subjects with dementia. Using linear methods of analysis, it has been shown that there is a slowing of the dominant rhythms in AD patients (Rosen 1996; Jonkman 1997). More recently, several groups have applied nonlinear dynamical analyses to EEG data from subjects

with probable AD (Jeong 2002). Nonlinear analyses have also been used to study neural processing in contexts other than dementia. In particular, a nonlinear metric, phase coherence, has been used to study neuronal information processing and long distance communication among different areas of the brain (Zhang et al., 2009a, 2009b). Other theoretical studies, also not specifically related to AD, have discussed the roles of different frequencies in information transfer in the brain (Kopell et al., 2000), and, in particular, have implicated the β band as an important frequency band for the transfer of information over long distances in the brain. A recent MEG study reported increased synchronization of resting-state functional connectivity over the parieto-occipital area in β band for AD patients (Stam et al., 2006).

Here we study phase coherence from EEG measurements of subjects with probable AD and compare the results with similar measurements on normals. We focus here on the photic-driven state. As we show, our study revealed a larger value of phase coherence among posterior electrodes during photic-driving in AD subjects than in normal control subjects. Unlike the MEG resting-state study, we find increased phase coherence among posterior electrodes across all frequency bands. This increased phase coherence is not seen very strongly in the anterior regions of the brain. We also present some preliminary results which suggest that the increase in posterior phase coherence may form the basis for an inexpensive, noninvasive robust biomarker for AD.

3.2 Methods

3.2.1 Patients and Data

Eight patients with mild to moderate dementia due to probable AD (mean age 75.5 years, SD 9.0; 4 males) and 6 normal control subjects (mean age 82.2 years, SD 6.2; 4 males) were recruited from the Alzheimer's Disease Research Center at the University of Michigan. The clinical diagnosis of probable AD was made according to the NINDS-ADRDA criteria (McKhann et al., 1984). Normal subjects were also examined by a neurologist and found to be cognitively intact. A two sample t-test showed there was no statistical difference between the age of AD and normal group ($t[12]=1.55$, $p=0.146$). All subjects were examined according to a clinical protocol, which included a 25-minute routine scalp EEG recording with intermittent photic stimulation (IPS). This single-site study was IRB-approved at the University of Michigan and all subjects gave informed consent.

EEG signals were recorded on a 128 channel BMSI/Nicolet 5000 system sampling at 250 Hz. The band pass was 0.1 to 70 Hz. 21 Scalp electrodes were placed according to the standard 10-20 International System (Jasper 1958). The reference electrodes used were A1 and A2, with a calculated common reference. The EEG was recorded for 25 minutes, with the subject in the alert or drowsy state. During the scalp EEG recording, a 220 second period of IPS was carried out, in which nonpathological responses, unusual responses, as well as abnormal responses were monitored, e.g. photic driving or photomyogentic responses, photoparoxysmal responses, and photosensitive epileptic seizures. For all the subjects, no unusual or abnormal response was found. IPS was administered with a stroboscopic source

placed 30cm from the patient in dim ambient light (barely sufficient for the examiner to discern the subject). The luminance of the source was 1,363 cd/m^2, and IPS was administered in 11 20-second cycles of stimulation at 2, 4, 6, 8, 10, 12, 14, 16, 20, 24 and 30 Hz.

The digital data were transferred to binary format for further analysis. The EEG was reviewed by a board certified clinical neurophysiologist who noted the beginning and end of IPS. To eliminate spatial overlap, 16 electrodes of clinical interest were selected for analysis, excluding midline electrodes Fz, Cz, Pz and ear electrodes A1 and A2.

3.2.2 Linear and Nonlinear Metrics

In this study, we used the nonlinear metric, phase coherence, for the purpose of studying brain nonlinear dynamics. The mathematical definition of phase coherence has been introduced in details in Chapter 1. The simple linear metric we used is cross correlation between a pair of signals $x_1(t)$ and $x_2(t)$, which is defined as

$$c = \frac{< A_1 A_2 >}{\sqrt{< A_1^2 >< A_2^2 >}} \tag{3.1}$$

where A_1 and A_2 are the amplitudes of the two signals The value of the cross correlation is bounded between 1 and -1, where 1(-1) indicates maximum correlation (anti-correlation) and 0 indicates no correlation.

3.2.3 Statistical Models

The primary purpose of this study is to evaluate differences between AD patients

and normal controls during photic stimulation. The EEG data was filtered into eight frequency bands: δ (1-4 Hz), θ (4-7 Hz), α_1 (7-10 Hz), α_2 (10-13 Hz), β_1 (13-18 Hz), β_2 (18-30 Hz) and γ (30-37 Hz), and the broad-band signal, 1-37 Hz. Again we used an order 5 band-pass Butterworth filter. Phase coherence values were computed for each 20-second window (5000 data points) during IPS, i.e., 11 values were calculated for 220 seconds of IPS data. We adopted a linear mixed model, which is an extension of the generalized linear regression model (GLM) that supports longitudinal data analysis by estimating fixed effects associated with the covariance structure of temporal correlations (Fitzmaurice et al., 2004). In this study, we chose the compound symmetric covariance structure which gave a more satisfactory AIC criterion.

Four groups of electrode pairs of clinical interest are sketched in Figure 3-1. The linear mixed model was repeated for 32 combinations of 8 frequency bands and 4 electrode pair groups.

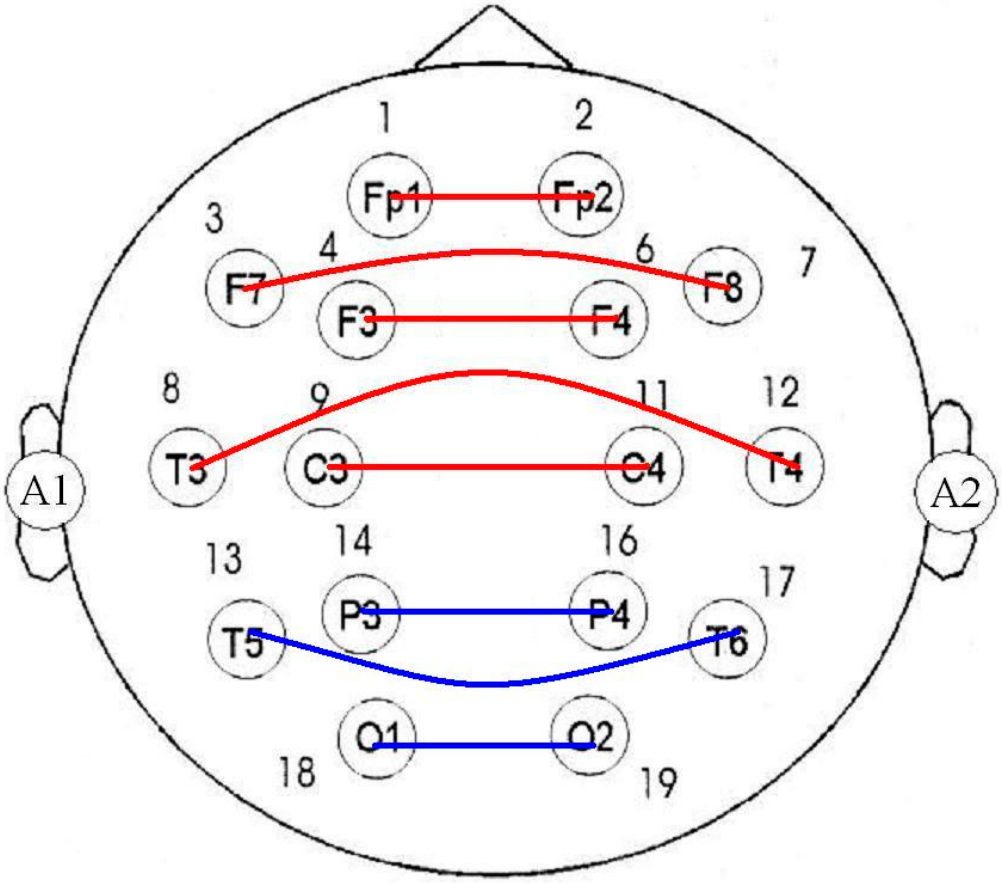

Figure 3-1a. Homologous long range pairs (red: anterior homologous pairs; blue: posterior homologous pairs)

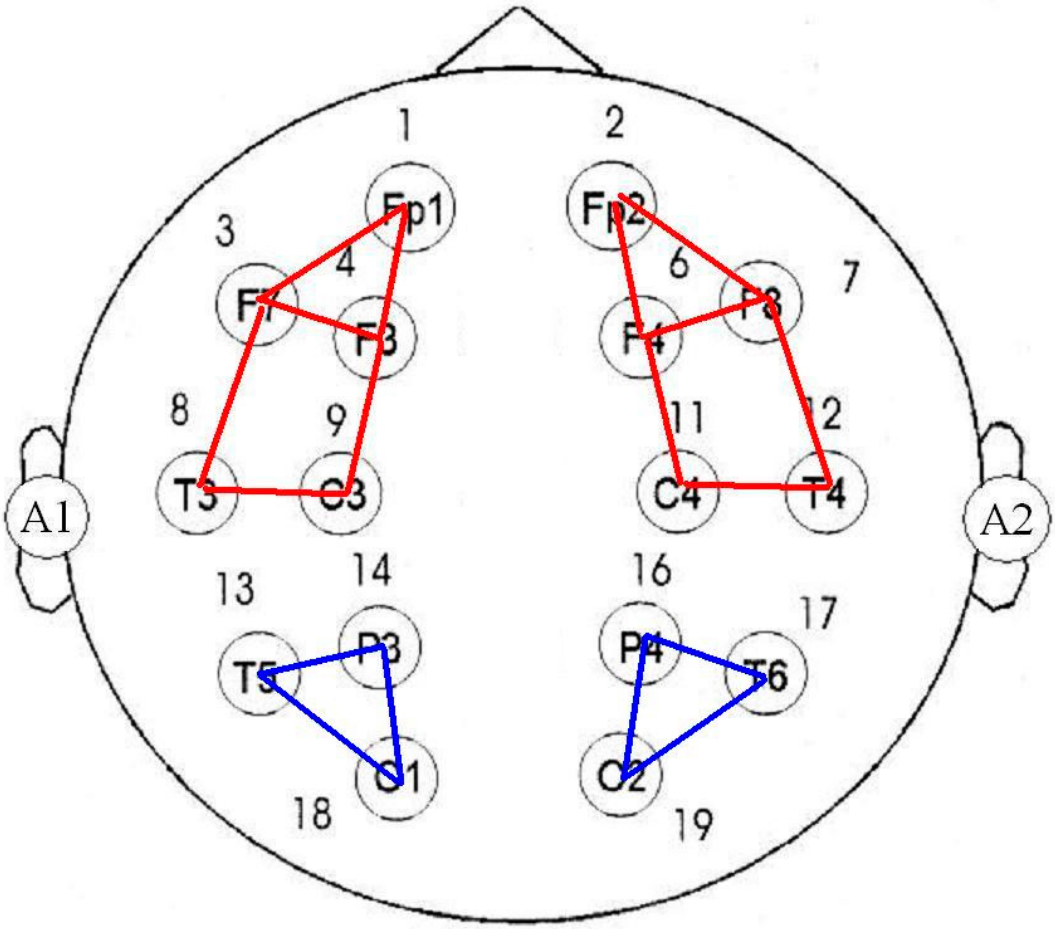

Figure 3-1b. Local short range pairs (red: anterior local pairs; blue: posterior local pairs).

Model 1: Phase coherence as a function of patient group and electrode pair location (for data from a group of electrode pairs).

$$\rho = a_0 + a_1 G + \sum_{i=1}^{n} b_i P_i \qquad (3.2)$$

where a_0 is the estimated intercept of normal controls, a_1 is the estimated intercept difference between AD patients and normal controls, G is the group indicator (G=0 for normal controls; G=1 for AD patients), b_i (i=1…n) are correction terms of electrode pairs, P_i (=0 or 1 for i=1…n) are indicators of each electrode pair, and n is the number of electrode pairs for each pair group (12 for the anterior local group, 5

for the anterior homologous group, 6 for the posterior local group and 3 for the posterior homologous group). This model was repeated for both phase coherence and cross correlation during IPS (11 windows).

Model 2: Mean phase coherence as a function of patient group (for data of a single electrode pair).

$$\rho = a_0 + a_1 G \tag{3.3}$$

where a_0 is the estimated intercept (estimated value of normal controls), and a_1 is the estimated difference between AD patients and normal controls. For each posterior local pair, this model was repeated for 8 frequency bands for both phase coherence and cross correlation. All statistical analyses were performed by SAS statistical software, version 9.1 (SAS Institute Inc., Cary, NC). As is standard, we rejected the null hypothesis (with 95% confidence) only if the associated p-value ≤ 0.05.

3.3 Results

3.3.1 Phase Coherence during Photic Driving

Estimated differences and associated p-values between AD patients and normal controls are presented in Table 3-1. Positive coefficient estimates indicate higher phase coherence during IPS in AD patients. Compared to normal controls, phase coherence values are higher for AD patients in 27 out of 32 combinations of frequency band and pair group. The posterior local pair group has significant increases in AD patients for almost all the frequency bands. Significant p-values were observed in δ, θ, α_1, α_2, β_1 and broad band. In the β_2 and γ bands, p-values are

not significant but are close to the 0.05 criterion. Other electrode pair groups have one or two significant increases in the δ band and/or broad band. Estimated phase coherence values seem to be lower for AD patients in 5 combinations: α_1, β_1, β_2 and γ bands for anterior homologous pairs and α_1 band for anterior local pairs. However, none of these differences is significant, and the estimated decreases are smaller in magnitude compared to the increases in phase coherence seen in posterior pairs.

	Anterior Homologous		Anterior Local		Posterior Homologous		Posterior Local	
	Difference	P-value	Difference	P-value	Difference	P-value	Difference	P-value
δ	**0.039**	**0.002**	**0.025**	**0.001**	**0.041**	**0.014**	**0.031**	**0.006**
θ	0.003	0.830	0.001	0.972	0.009	0.551	**0.033**	**0.003**
α_1	-0.003	0.823	-0.008	0.384	0.005	0.775	**0.024**	**0.039**
α_2	0.008	0.485	0.006	0.475	0.021	0.133*	**0.038**	**0.004**
β_1	-0.004	0.748	0.011	0.242	0.001	0.966	**0.027**	**0.011**
β_2	-0.004	0.851	0.014	0.264*	0.007	0.674	0.022	0.157*
γ	-0.002	0.943	0.016	0.309	0.010	0.596*	0.033	0.073*
Broad	**0.024**	**0.048**	**0.032**	**0.001**	0.022	0.132*	**0.037**	**0.001**

Table 3-1. Difference in mean phase coherence values between AD patients and normal controls during IPS (Positive difference indicates higher phase coherence in AD patients; Bold represents statistical significance ($p \leq 0.05$); *: Additional significant p-values for cross correlation during IPS).

3.3.2 Cross Correlation during Phtoic Driving

The results of mean cross correlation differences during IPS were qualitatively similar to the results seen in phase coherence. (However, the standard deviations of the cross correlations was substantially higher than the standard deviations for phase coherence differences. This is likely to be an important consideration when considering the development of biomarkers for AD: Higher standard deviations will result in a less robust biomarker.) Six electrode group/frequency band combinations which do not show significant differences in phase coherence do show significant differences in cross correlation. (Table 3-1, marked by asterisk). They are β_2 band of anterior local pairs, α_2, γ and broad band of posterior homologous pairs, and β_2 and γ band of posterior local pairs. Both phase coherence and cross correlation are higher for AD subjects in these groups, although only the cross correlation measurements are statistically significant.

3.3.3 Phase Coherence in a Single Posterior Pair during Photic-driving

Estimated differences in phase coherence during photic-driving for a single posterior local pair (model 2) were computed. No significant p-values were detected. Despite the absence of statistical significance in model 2, it is worthwhile exhibiting qualitative trends in differences between AD and normal subjects. To this end, we show in Table 3-2 the percent differences between AD patients and normal controls (calculated as (AD-Normal)/Normal). These are divided into three categories: 1. small positive changes (0% - 15%); 2. large positive changes (over 15%); 3. small

negative changes (0% - 15%). The estimated differences of pair T5-O1 are over 15% for all the frequency bands, with the two largest increases in the γ band (35%) and broad band (33%). No other electrode pair has over 30% larger phase coherence in AD patients compared to normals. Below, we will use the phase coherence differences in the T5-O1 pair in the γ band and broad band during IPS to construct a trial biomarker for AD. We will also compare the use of T5-O1 to averages over posterior local pairs as a biomarker.

	δ	θ	α_1	α_2	β_1	β_2	γ	Broad
P3-T5	-	+	+	+	+	+	+	+
P3-O1	+	+	+	*	*	+	+	*
T5-O1	*	*	*	*	*	*	+35%	+33%
P4-T6	+	+	+	+	+	-	-	+
P4-O2	*	+	*	*	*	+	+	*
T6-O2	*	+	+	+	+	+	*	*

Table 3-2. Estimated difference of mean phase coherence between AD patients and normal controls for posterior local pairs during IPS (+: 0 - 15% increase in AD patients; *: Over 15% increase in AD patients; -: 0 – 10% decrease in AD patients)

3.4 Discussion

A general pattern of increased synchrony during photic-driving for AD patients, particularly among posterior electrode, compared to normals was observed in this study. Both phase coherence and cross correlation during IPS were larger in AD patients than in normal subjects in most frequency bands for posterior local pairs. For the purposes of exploring biomarkers based on scalp EEG data, we have also examined the use of synchrony measurements from a single pair of posterior

electrodes as potential biomarkers for AD.

The data of each posterior local pair was investigated using Model 2. Among all the combinations of posterior local pair and frequency band, we found that the γ band and broad band phase coherence of pair T5-O1 have the highest increases in percentage. The broad band phase coherence of T5-O1 is given in Figure 3-2a. Although the p-value is not significant at the 95% confidence level, it is close (p=0.06). Using this data we have constructed an ROC curve measuring discrimination between AD and normal subjects using the average phase coherence values during photic-driving of the T5-O1 pair. This is shown in Figure 3-2b. The area under the ROC curve (AUC) is 0.80. In Figure 3-2c, we present the γ band phase coherence of T5-O1. The associated ROC curve for the γ band phase coherence is shown in Figure 3-2d. The area under this ROC curve is 0.75. Although the area under the broad band ROC curve (Fig. 3-2b) is higher, the γ band phase coherence may be preferable as a biomarker for the lower false positive rate necessary to achieve a 75% true positive rate. In Figure 3-2c, we also notice a possibly anomalous result for one normal subject (dashed blue line, average=0.499), which is more than 3 standard deviations (0.086) higher than the group mean of the other 5 normal subjects (0.166). Since there are only 6 normal subjects, the impact of this single high phase coherence value is significant. After removal of this possible outlier, the γ band ROC curve achieves a 75% true positive with 0% false positive (Fig. 3-2d), and the area under the ROC curve becomes 0.90, which is generally considered excellent accuracy for a diagnostic test. These results suggest

that both the γ band and broad band phase coherences are potential biomarkers for AD. However, given our small sample size, it is important to emphasize that we do not *necessarily* suppose that this particular combination of electrode pair and frequency ranges will be optimal once more data is available. Clearly, a much larger sample size is necessary to validate either of these metrics (or related ones) as useful AD biomarkers.

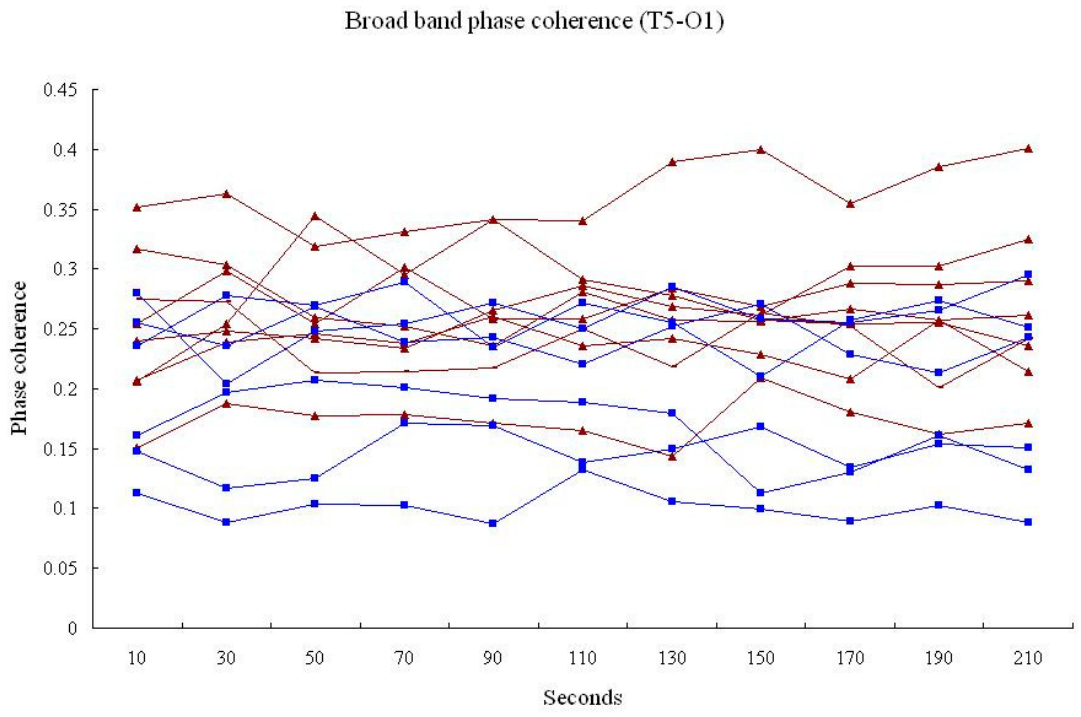

Figure 3-2a. T5-O1 broad band phase coherence values (brown: AD patients; blue: normal controls).

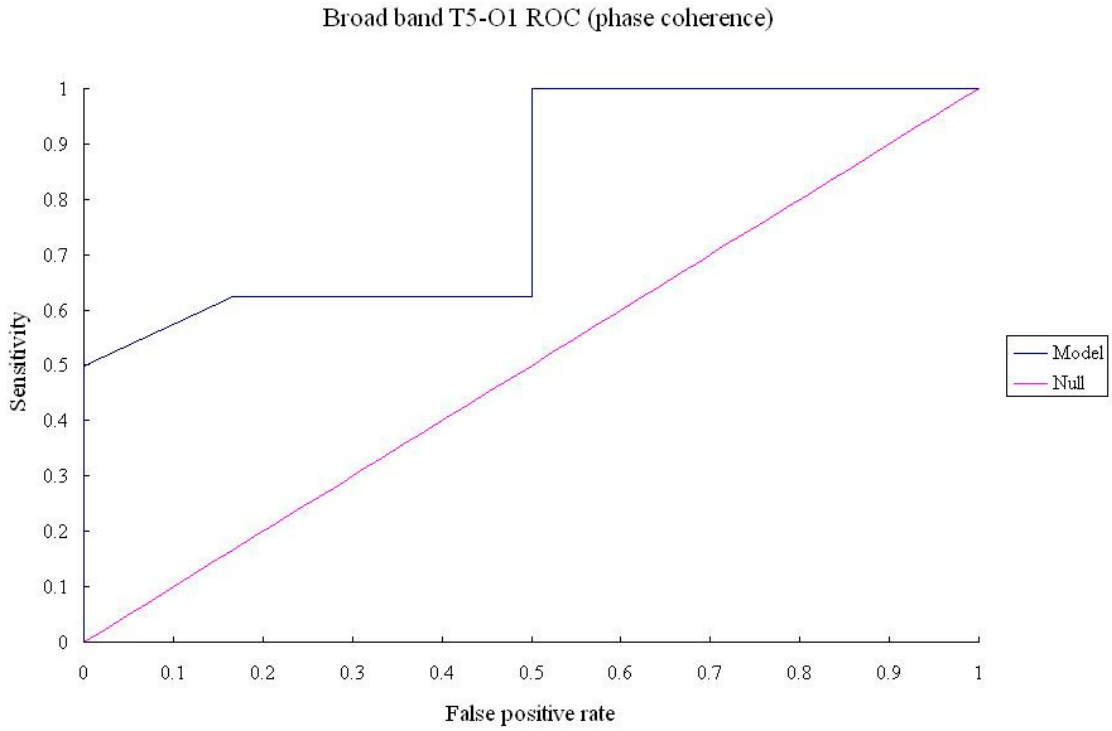

Figure 3-2b. T5-O1 broad band phase coherence ROC curve (blue) compared to the null (pink).

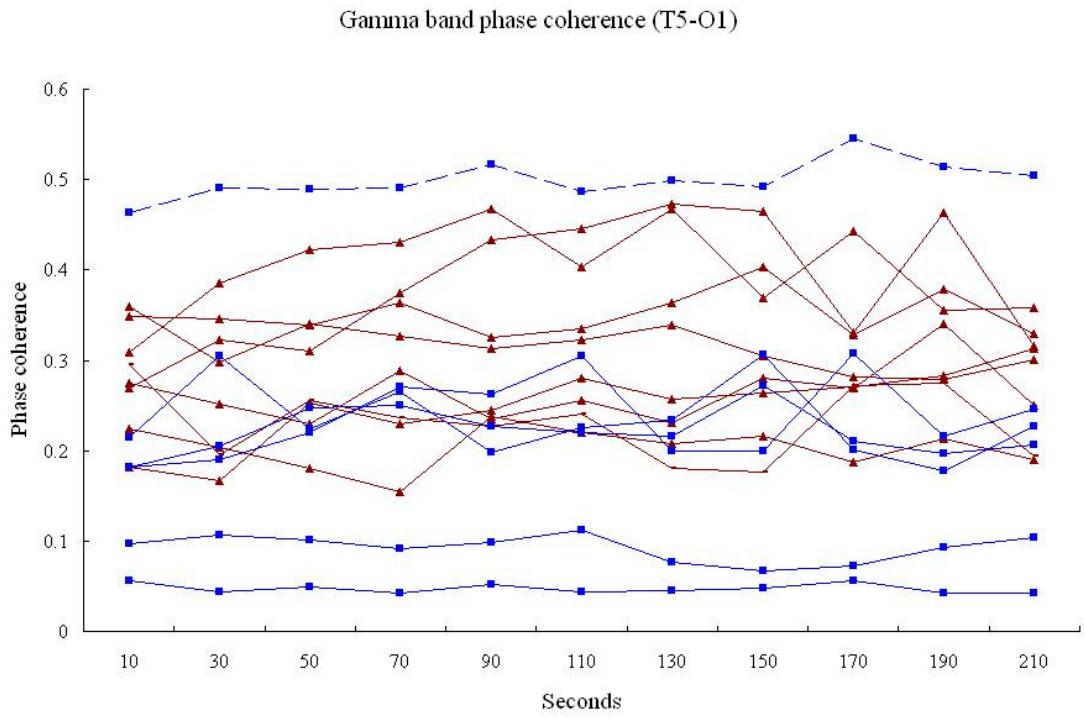

Figure 3-2c. T5-O1 gamma band phase coherence values (brown: AD patients; blue: normal controls; blue dashed: the suspicious normal subject whose mean value exceed 3 standard deviations of group mean).

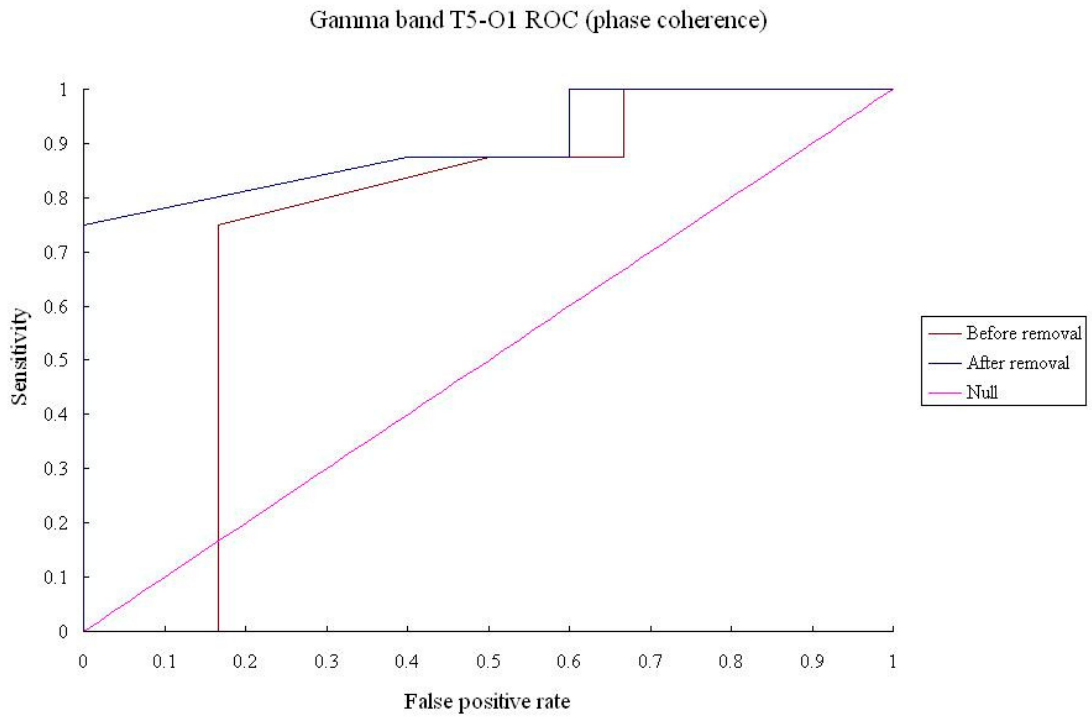

Figure 3-2d. T5-O1 gamma band phase coherence ROC curves (brown: using the data of all normal subjects; blue: eliminating the suspicious normal subject whose mean value exceed 3 standard deviations of group mean) compared to the null pink.

An interesting question from both a practical and theoretical point of view is whether nonlinear dynamical metrics (e.g., phase coherence) add new information not contained in linear metrics (e.g., cross correlation). This is a particularly interesting question in the context of our discussion of potential biomarkers. Recall that in Table 1 we found increased synchronization in AD patients using both phase coherence and cross correlation in statistical models in most frequency bands of posterior local pairs. On the other hand, in Figures 3-2 and 3-3 we showed that phase coherence has the potential to effectively distinguish between AD and normal subjects. We now investigate the γ band (Fig. 3-3a and 3-3b) and broad band (Fig.

3-3c and 3-3d) cross correlation of pair T5-O1, (the most promising frequency/pair combinations using cross-correlation) and compare the efficacy of cross correlation with phase coherence as potential AD biomarkers. The area under the ROC curve associated with the γ band cross correlation is 0.63 (Fig. 3-3b), lower than the result using γ band phase coherence. Furthermore, in Figure 3-3a there appears to be no obvious difference between AD patients and normal controls, except for an extremely low cross correlation in two normal subjects. The broad band cross correlation of T5-O1 is given in Figure 3-3c. The area under the ROC curve associated with broad band cross correlation is 0.74, somewhat lower than the area under the ROC curve using broad band phase coherence (0.80). Moreover, the ROC curve of broad band phase coherence is an upper envelope of the ROC curve of broad band cross correlation. Thus, from this limited sample size, the nonlinear metric of phase coherence appears to have more potential as a biomarker for AD than does the linear metric of cross correlation.

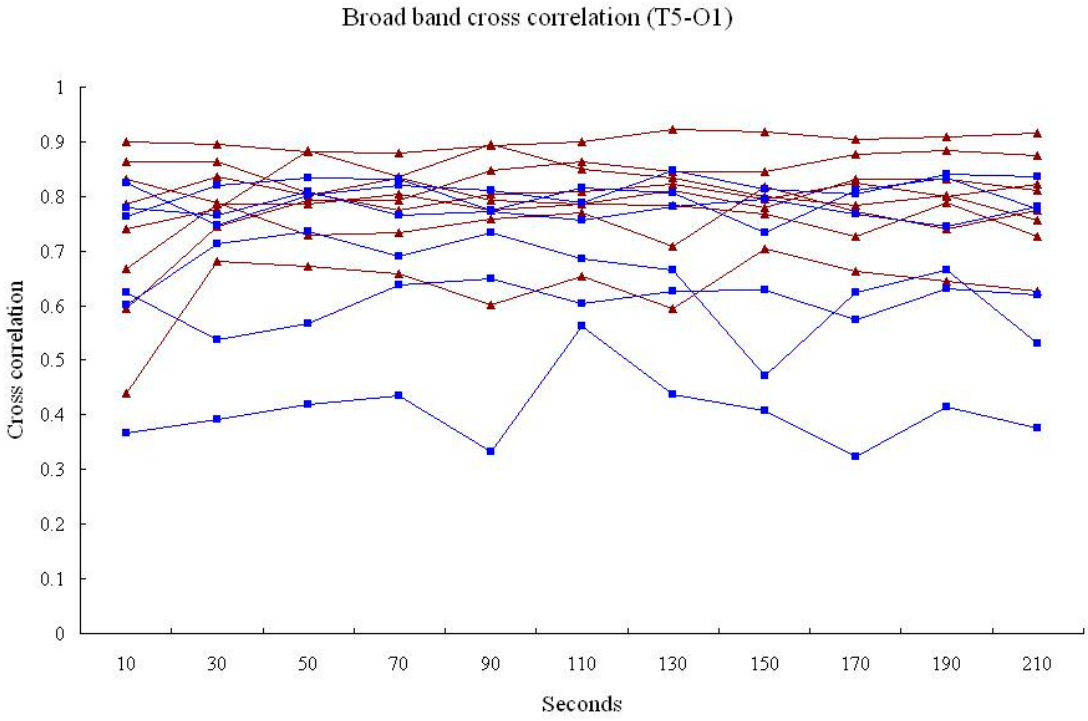

Figure 3-3a. T5-O1 gamma band cross correlation values (brown: AD patients; blue: normal controls; blue dashed: suspicious normal control).

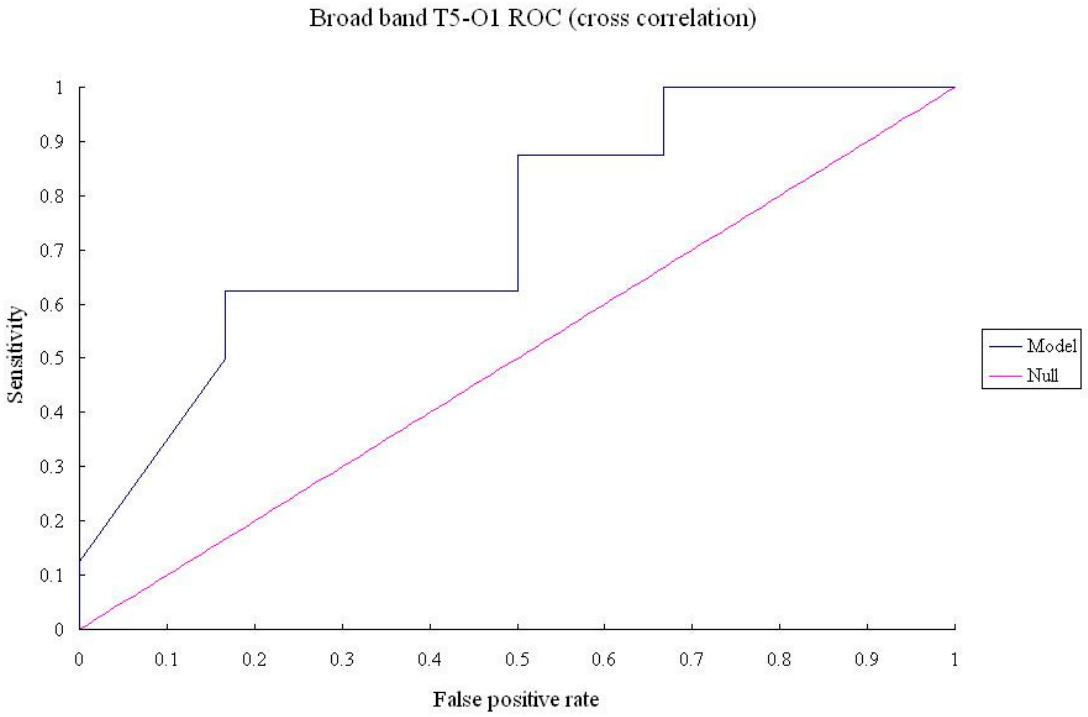

Figure 3-3b. T5-O1 gamma band cross correlation ROC curve (blue) compared to the null (pink)

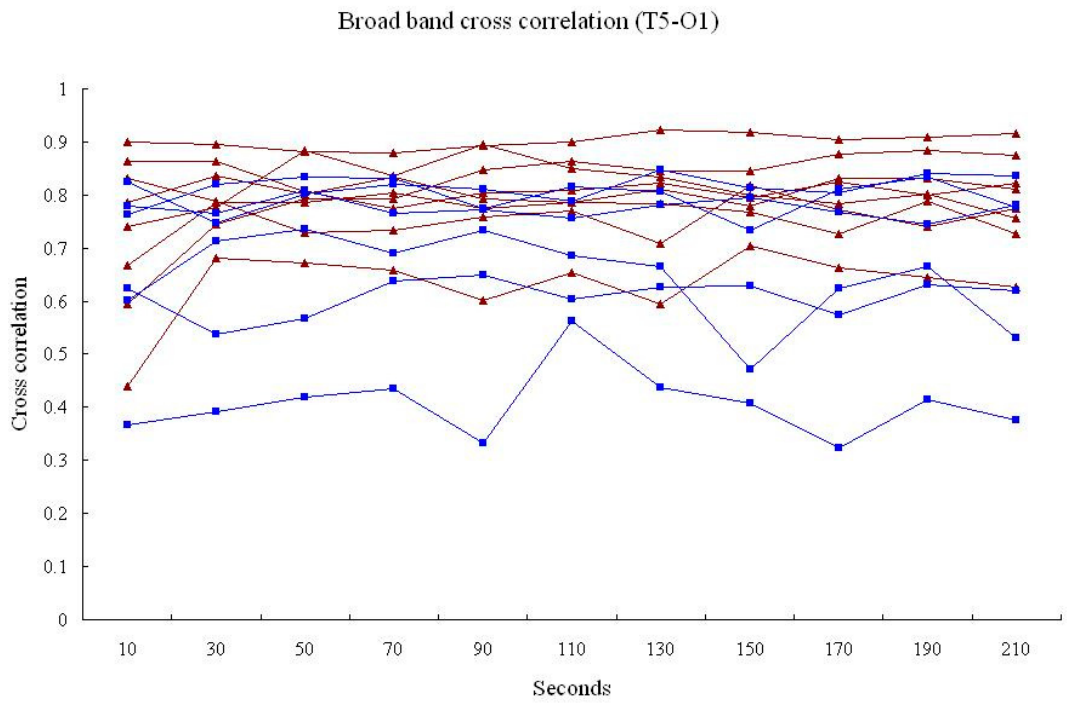

Figure 3-3c. T5-O1 broad band cross correlation values (brown: AD patients; blue: normal controls).

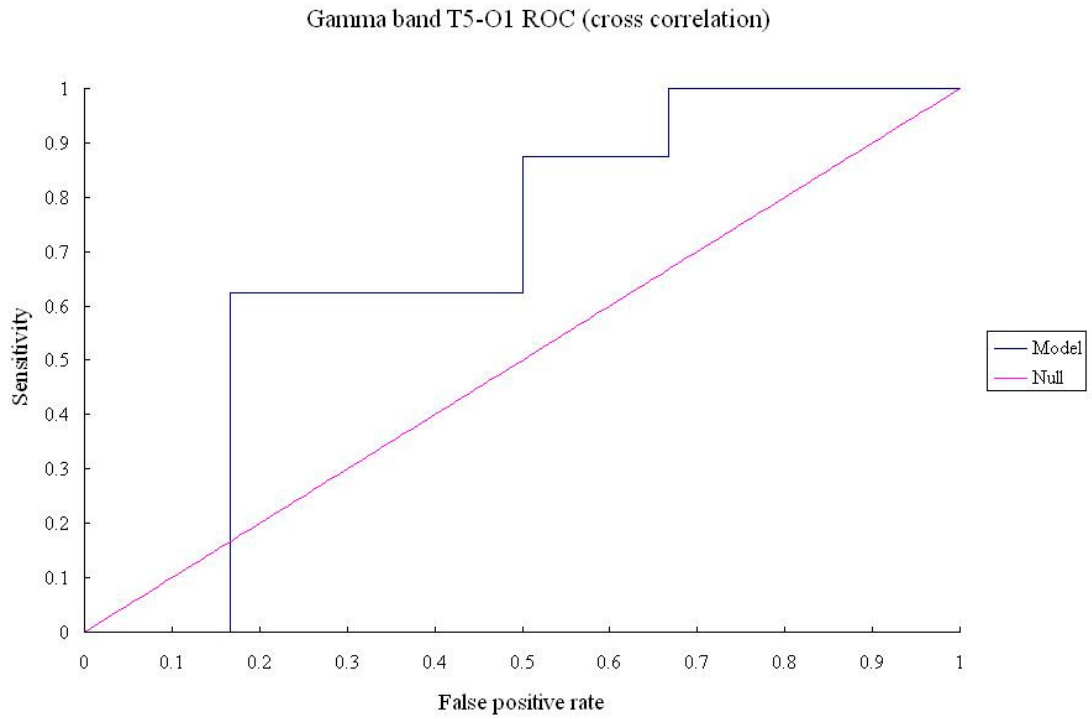

Figure 3-3d. T5-O1 broad band cross correlation ROC curve (blue) compared to the null (pink).

It is possible that the identification of the T5-O1 pair as the one with the maximum difference in phase coherence is a function of our small sample size. We therefore also consider differences in the average phase coherence of the posterior local pairs between AD patients and normals as another candidate biomarker. Since this biomarker uses six times the data of one based on a single electrode pair, it may be more stable and and least somewhat less susceptible to small sample bias. Using this average phase coherence, we repeated the γ band and broad band ROC curves. The areas under the new ROC curves are 0.76, 0.69 and 0.85 for broad band, γ band including the possible outlier, and γ band without the possible outlier, respectively. By comparison, the area under the ROC curves of the pair T5-O1, are 0.80, 0.75 and 0.90 respectively, so that the average phase coherence of posterior local pairs is

almost as efficacious as the best single pair phase coherence. However, it is possible that the observation that the highest increase in phase coherence is in pair T5-O1 may not be a small sample effect since the left hemisphere may be more susceptible that the right to neurodegeneration in Alzheimer's Disease. Recent studies of *in* vivo imaging of amyloid distribution using positron emission tomography (PIB-PET) have revealed a high amyloid burden in the parietal neocortex; this seems to correlate with regional hypometabolism as seen on FDG-PET imaging (Klunk et al., 2004). Furthermore, since there have been more frequently observed abnormalities in the left hemisphere of the brain for AD patients (Thompson et al., 1998; Knyazeva et al., 2008), our observation may have a physiological basis. The choice between single pair phase coherence and average phase coherence as the most efficacious biomarker for AD requires further analysis with a larger sample size.

In our study comparing AD patients and normals during photic stimulation, we have observed the strongest abnormalities over the parieto-occipital area. Although good resting-state data was not available for this study, other groups have observed some differences in the resting state between subjects with dementia and normals (Lustig et al., 2003). On the other hand, a recent EEG study reported that task-induced EEG changes may emphasize the difference between MCI subjects and controls (Van der Hiele et al., 2006). Since the resting-state network emphasizes the frontal, posterior cingulated, parietal and medial temporal areas (Laufs et al., 2003), differences between AD and normal controls over the parieto-occipital area may be more sensitive during some task-related events or during stimulation that affects

occipital cortex networks. Compared to a recent MEG study (Stam et al., 2006) which reported increased parieto-occipital synchronization likelihood (a nonlinear metric) in α_2, β and γ band during the eye-closed rest state for AD patients, we observed enhanced synchronization in almost all the frequency bands of phase coherence and cross correlation during IPS in this same brain region. It is also interesting to compare these observations with many of those summarized (Jeong 2002). The general picture that emerges from much previous work is a picture of decreased cerebral complexity in dementia, with a concomitant decrease in communication in the brain sometimes signaled by a decrease in metrics of communication such as correlations. Observations, such as ours, of higher in phase coherence in AD patients may therefore seem paradoxical. One possible explanation for such observations is that the general decreased complexity of the brain may lead, under conditions of stimulation, (such at photic stimulation) to a simpler cerebral response. That is, if the brains of dementia patients are, in general, less complex and more simply connected, much of the internal (structured) communication in the brain may be suppressed, so that portions of the brain associated with responses to external stimuli (in our case the occipital-parietal regions) may respond more uniformly to the external stimuli, resulting in the observation (using linear and nonlinear metrics) of greater synchrony. This hypothesis is consistent with the fact that AD afflicts primarily the multimodal association cortices subserving higher cognitive functions rather than (and superimposed upon) primary sensory (and motor) cortices subserving primary sensory modalities such as vision.

Most of the subjects with dementia in this study were diagnosed with probable AD. However, we also studied two subjects with frontotemporal dementia (FTD), in which portions of the frontal and temporal lobes shrink or atrophy. The results for the patients with FTD were similar to those with AD, but with some differences. Most notably, this small group of FTD patients had higher mean phase coherence among the local posterior electrodes than the AD patients in all frequency bands. This preliminary result might correspond to an interesting report by Seeley et al., 2008, in which the authors reported that a FTD patient who showed severe degeneration of the left inferior frontal-insular, temporal and striatal regions developed an intense drive to produce visual art. By using neuroimaging analyses, they found increased grey matter volume and hyperperfusion in the right posterior neocortical areas of the patient, which implicated heteromodal and polysensory integration in the non-dominant brain regions. The authors believed that structural and functional enhancement in non-dominant posterior neocortex may give rise to specific forms of visual creativity that can be liberated by dominant inferior frontal cortex injury. However, because of the very small sample size, no conclusions of statistical significance can be drawn. But these observations suggest that photic stimulation may also be useful as a biomarker for other types of dementia, and may even have utility to discriminate among different types of dementia. The veracity of these suggestions must await larger scale studies.

Finally, because of the potential dependence of phase coherence on the choice of reference electrode, we repeated all our calculations of photic-driven phase coherence

with two different reference schemes, the average of A1 and A2, and Fz. In general we found that choosing different EEG reference electrodes generated quantitatively different but qualitatively similar results. The only interesting difference when using Fz as a reference electrode was that there was no significant difference between AD and normals for anterior pairs in the δ band and in broad band. Since Fz may carry similar δ waves as other anterior electrodes, referencing to Fz might have reduced coefficient estimates and the statistical significance in δ band and broad band. Moreover, a bi-spectral analysis has demonstrated phase coupling between theta activity recorded at Fz and fast activity in the frontopolar regions during short-term memory tasks, suggesting that structures near Fz (eg. the cingulate gyrus) may modify fast oscillations in other cortical regions during information processing (Schack et al., 2002).

3.5 Summary

In conclusion, increased posterior phase coherence was observed in AD patients for all the frequency bands, with statistical significance in five out of seven bands, and near significance in the remaining two. Using mean phase coherence in the γ band for the T5-O1 pair as a biomarker for AD resulted in a 75% true positive rate together with a false positive rate that was only 0 to 16.7%, and the area under the ROC curve was 0.90 and 0.75 respectively. Since the completely random guess would give its prediction along the diagonal line from the left bottom to the right top corner (AUC=0.5), AUC=0.9 indicated excellent diagnostic performance for a potential

biomarker. It is likely that these rates can be substantially improved, but much larger additional studies will be required. Such studies will have to include tight control of potentially confounding factors such as medications and other existing health conditions. Our preliminary observations on FTD subjects also suggest that nonlinear metrics calculated from noninvasive EEG may have utility as biomarkers for other types of dementia, and encourages further studies to determine if such biomarkers can, additionally, be discriminative for distinguishing among various kinds of dementia. Furthermore, with the increased sensitivity and specificity that will come from additional studies such as these, it also possible to imagine the development of inexpensive diagnostic procedures that can distinguish between impending dementia and other underlying conditions in patients with mild cognitive impairment (MCI).

CHAPTER 4

EPILOGUE

In our study, we used scalp EEG to examine brain activities for both temporal lobe epilepsy and Alzheimer's disease. We applied a nonlinear dynamic metric, phase coherence, to measure the synchronization of cellular activities. The linear mixed models were implemented to correlate the changes in repeated phase coherence measures controlling for brain wave frequency, state of consciousness, epileptic state (interictal and preictal), and anatomical position of EEG electrodes.

For patients with temporal lobe epilepsy, our results suggested a lack of information transfer of the brain in epilepsy patients during interictal periods, but not during preictal periods. In particular, we found increased phase coherence in the anterior region compared to the posterior region in the preictal periods, in agreement with experimental observation that seizures mainly propagate through the anterior region of the brain. For Alzheimer's disease, our results indicated significant increases in both phase coherence and cross correlation in posterior local pairs of AD patients compared to normal subjects during the intermittent photic stimulation (IPS) task. Anterior pairs did not show such a marked difference. Using mean phase coherence in the γ band for the T5-O1 pair as a biomarker for AD resulted in a 75% true positive rate together with a false positive rate that was only 0 or 16.7% (excluding or including the potential outlier in normal subjects).

Our detailed study of phase coherence in scalp EEG data had three important implications. First, it improves our understanding of seizure generation and propagation in temporal lobe epilepsy. In this study we have shown significant lower phase coherence measured from pairs of scalp electrodes in subjects with temporal lobe epilepsy during interictal epochs, compared to measurements in normal subjects. We have also shown that phase coherence levels increase during preictal epochs, approaching levels found in normal subjects. These general trends were suggestive of an intriguing general dynamic that may be important in seizure propagation.

Second, our research indicates that nonlinear time series analysis carries features from brain electrical activity. By using the linear mixed model, we have demonstrated that phase synchronization during preictal periods differ clearly from interictal periods under various combinations of frequency bands and behavior states, after controlling for electrode location. Our results were also qualitatively consistent with various choices of reference electrode. Differences were most pronounced for theta, alpha-2, and beta-2 bands during awake, stage 1 and stage 2 sleep among anterior electrode pairs. This work may lay the groundwork for the development of a non-invasive, reliable method of seizure prediction. If one is able to predict seizures reliably, one may be able to develop acute therapies that can be used to abort the seizures. This will be a major step forward in the treatment of epilepsy, particularly for those patients whose conditions are medically intractable.

Third, our observation of statistically significant increases in phase coherence

served well as a potential biomarker for AD. During the 220-second IPS epoch, we have observed the maked differences between normals and subjects with probable AD over the parieto-occipital area, for almost all the frequency bands studied. It is likely that the sensitivity can be further improved with additional studies using larger sample size. For example, potential risk factors may be better controlled by using exact age and gender matched control subjects, and including probable lesion areas of the brain. It would also be interesting to study differences in phase synchronization during the resting-state, and compare those results with the ones obtained during IPS. It would also be interesting to test phase coherence as a biomarker for other types of dementia. In a preliminary data analysis, we also found increased mean phase coherence in FTD and MCI subjects. However, these results were not statistically significant due to the limit of a small sample size. The veracity of these suggestions awaits larger scale studies.

Abnormalities in scalp EEG recordings from patients with neurological diseases have been extensively studied in the past decades. The role of nonlinear time series analysis is becoming more important, with numerous results from studying nonlinear dynamics in complex behaviors of brain electrical activity. However, many issues remain to be more fully investigated, including artifact effects on nonlinear dynamics, discrepancies between results from intracranial EEG, drug effect on neurodynamics, and the association between cognitive performance and nonlinear EEG dynamics. Further studies regarding to these questions would contribute to a deeper understanding of the mechanisms of neuropathological EEG recordings.

APPENDICES

Appendix 1. Wilcoxon Rank-Sum Test

The Wilcoxon rank-sum test (or Mann-Whitney test) is a non-parametric test based solely on the order of values from two random samples X and Y (Lehmann 1975). If the two samples come from the same distribution and the values are drawn randomly for both samples, then the values in the two different samples should be somewhat equally distributed.

For example, assume $X_1, \ldots, X_{n1}$ in sample X are drawn from distribution F_X; $Y_1, \ldots, Y_{n2}$ in sample Y are drawn from distribution F_Y. The null hypothesis H_0 is $F_X = F_Y$. The test is calculated in the following way:

1. Combine the two samples into one sample W_i, where i =1, 2, …, n_1+n_2 and in the combined sample $W_{(1)} \leq W_{(1)} \leq \ldots \leq W_{(n1+n2)}$
2. Assign rank *i* to the i^{th} smallest value (assign the average rank in case of ties)
3. Let R_X = sum of ranks attached to values in sample X
4. Statistic $U=\max(K, n_1n_2 - K)$, where $K = R_X - n_1(n_1-1)/2$
5. Find distribution of U_0 under H_0, and reject H_0 if $P(U_0 \geq U) \leq \alpha$

Compared to parametric tests (such as the t-test), the advantage of the Wilcoxon rank-sum test is that it does not take any ancillary assumptions of the distribution of sample X and Y, which gives a lot of flexibility in comparing two samples drawn independently from unknown distributions.

Appendix 2. The Linear Mixed Model

The linear mixed model is an extension of the generalized linear regression model (GLM), which supports longitudinal data analysis by estimating fixed effects with covariance structures of temporal correlation (Fitzmaurice et al., 2004). It is also applied in analysis of continuous dependent variable with random effects and hierarchical effects. Coefficient estimate and statistical inference of the linear mixed model can be derived using weighted least squares or the maximal likelihood method. The Laird-Ware (matrix) form of the linear mixed model is given as follows (Laird and Ware 1982):

$$\boldsymbol{y_i} = \boldsymbol{X_i\beta} + \boldsymbol{Z_i b_i} + \boldsymbol{\varepsilon_i}$$

$$\boldsymbol{b_i} \sim N_q(0, \boldsymbol{\Psi})$$

$$\boldsymbol{\varepsilon_i} \sim N_{ni}(0, \boldsymbol{\sigma^2 \Lambda_i})$$

where $\boldsymbol{y}$ is response vector for observations, $\boldsymbol{X}$ is the matrix of fixed-effect observations, $\boldsymbol{\beta}$ is the vector of fixed-effect coefficients, $\boldsymbol{Z}$ is the matrix of random effects, $\boldsymbol{b}$ is the vector of random effect coefficients, $\boldsymbol{\varepsilon}$ is the vector of errors, $\boldsymbol{\Psi}$ is covariance matrix of random effects, $\boldsymbol{\sigma^2 \Lambda}$ is the covariance matrix of residuals and the subscript, i, is the subject index.

Since statistical inference of longitudinal data requires nonzero off-diagonal terms in the residual covariance matrix, a compound symmetry type of covariance structure is adopted for simple consideration of temporal correlation in our paper. Random effect is only considered for the intercept.

BIBLIOGRAPHY

Akaike H, 1969. Power Spectrum Estimation Through Autoregressive Model Fitting. Annals of the Institute of Statistical Mahtematics, Vol 21, 407-419.

Armitage P, Berry G (1994) Statistical Methods in Medical Research. Blackwell.

Bhattacharya J (2001) Reduced degree of long range phase synchrony in pathological human brain. Acta Neurobiol Exp. 61, 309-318.

Begley et al., (2000) The cost of epilepsy in the United States: an population-based clinical and survey data, Epilepsia 41, 342-351

Bendat J.S., Piersol A.G. (2000) Random Data, Analysis and Measurement Pro-cedure. John Wiley & Sons Inc., New York

Brock W, Dechert W, Scheinkman J. (1987) A test for independence based on the correlation dimension. Working paper, Department of Economics, University of Wisconsin, Madison.

Dominguez LG, Wennberg RA, Gaetz W, Cheyne, D, Snead III, OC, Velazquez, J (2005) Enhanced Synchrony in Epileptiform Activity? Local versus Distant Phase Synchronization in Generalized Seizures. Journal of Neuroscience. 25(35).

Drury I, Li D, Savit, R (2003) Seizure Anticipation Using Scalp EEG. Journal of Experimental Neurology. 184 (supplement 1), 9.

Duke F, Pritchard D. Measuring Chaos in the Human Brain, World Scientific, Singapore, 1991.

Fitzmaurice, G., Laird N. and Ware J., (2004) Applied Longitudinal Analysis. Wiley Interscience.

Fuster JM. Cortex and Mind. Unifying Cognition. Oxford Univ. Press, New York, 2003.

Gonzalez-Portillo G, Rivero S, Ahern GL, Labiner DM, and Weinand ME.(2004), Normalization of periictal bihemispheric cerebral perfusion in temporal lobe epilepsy, Pathophysiology, 11:31-34

Grassberger P, Procaccia I (1983) Measuring the strangeness of strange attractors. Physica D 9: 189–208.

Guevara R, Velazquez JL, Nenadovic V, Wennberg R, Senjanovic G, Dominguez LG (2005) Phase synchronization measurements using electroencephalographic recordings: what can we really say about neuronal synchrony? Neuroinformatics. 3:301–314.

Iasemidis L, et al., Nonlinear dynamics of ECoG data in temporal lobe epilepsy. Electroencephalogr Clin Neurophysiol 1988;5:339.

Jasper HH (1958) Report of the committee on methods of clinical examination in electroencephalography. Electroencephalogr Clin Neurophysiol. 10: 370-375.

Jelles B, Strijers RL, Hooijer C, Jonker C, Stam CJ, Jonkman EJ. 1999a. Nonlinear EEG analysis in early Alzheimer's disease. Acta Neurol Scand 100:360–368.

Jeong J, Kim SY, Han SH. 1998. Non-linear dynamical analysis of the EEG in Alzheimer's disease with optimal embedding dimension. Electroencephalogr Clin Neurophysiol 106:220–228.

Jeong J, Gore J, Peterson B. Mutual information analysis of the EEG in patients with Alzheimer's disease. 2001, Clinical Neurophsiology 112, 827-835

Jeong J. Nonlinear dynamics of EEG in Alzheimer's Disease. Drug Development Research 2002; 56: 57–66.

Jonkman EJ. The role of the electroencephalogram in the diagnosis of dementia of the Alzheimer type: an attempt at technology assessment. Neurophysiol Clin.1997; 27: 211–219.

Kandel E, Schwartz J, Jessell T, (2000) Principles of Neural Science, McGraw-Hill Medical.

Klunk WE, Engler H Nordberg A, Wang Y Blomqvist G, et al., Imaging brain amyloid in Alzheimer's disease with Pittsburgh compound-B. Ann Neurol 2004;55:306-319.

Knyazeva MG, Jalili M, Brioschi A, et al., Topography of EEG multivariate phase synchronization in early Alzheimer's disease. Neurobiology of Aging, articles in press, 2008.07.019.

Kopell N, Ermentrout G, Whittington M, Traub R (2000) Gamma rhythms and beta rhythms have different synchronization properties. Proceed Nat Acad Science. 97, 1867.

Laufs H, Krakow K, Sterzer P, et al., Electroencephalographic signatures of attentional and cognitive default modes in spontaneous brain activity fluctuations at

rest. Proc Natl Acad Sci. 2003; 100: 11053–11058.

Lehmann E, Nonparametrics: Statistical Methods Based on Ranks, Holden-Day, Oakland, 1975.

Lustig C, Snyder AZ, Bhakta M, et al., Functional deactivations: change with age and dementia of the Alzheimer type. Proc Natl Acad Sci. 2003; 100, 14504–14509.

Lehnertz K, C.E. Elger, Spatio-temporal dynamics of the primary epileptogenic area in temporal lobe epilepsy characterized by neuronal complexity loss, Electroencephalogr. Clin. Neurophysiol. 95 (1995) 108–117.

Lehnertz K, Elger C. Can epileptic seizures be predicted? Evidence from nonlinear time series analysis of brain electrical activity Phys Rev Lett. 1998;80:5019–22.

Lehnertz K, Arnhold J, Grassberger P, Elger CE, eds. Chaos in brain? Singapore, World Scientific, 2000.

Lehnertz K, et al., EEG nonlinear analysis in epilepsy. J Clin Neurophysiol 2001;18:209–22.

Le Van Quyen, M., Martinerie, J., Baulac, M. and Varela, F. (1999) "Anticipating epileptic seizures in real time by a non-linear analysis of similarity between EEG recordings", NeuroReport 10, 2149-2155

Le Van Quyen M, C. Adam, J. Martinerie, M. Baulac, S. Clemenceau, F. Varela, Spatio-temporal characterizations of non-linear changes in intracranial activities prior to human temporal lobe seizures, Eur. J. Neurosci. 12 (2000) 2124–2134.

Le Van Quyen, M., Foucher, J., Lachaux, J., Rodriguez, E., Lutz, A., Martinerie, J. and Varela, F.J. (2001) Comparison of Hilbert transform and wavelet methods for the analysis of neuronal synchrony, Journal of Neuroscience Methods 111:83-98

Li D, Zhou W, Drury I, and Savit R. (2003a) "Nonlinear, Non-invasive Method for Seizure Anticipation in Focal Epilepsy", Mathematical Biosciences, 186; 63-77.

Li D, Zhou W, Drury I, and Savit R. (2003b) "Linear and Nonlinear Measures and Seizure Anticipation in Temporal Lobe Epilepsy", Journal of Computational Neuroscience 15, 335.

Li D, Zhou W, Drury I, Savit R (2006) Seizure Anticipation, States of Consciousness and Marginal Predictability in Temporal Lobe Epilepsy. Epilepsy Research. 68, 9.

Manuca, R., and Savit, R. (1996). Stationarity and nonstationarity in time series

analysis, Physica D, 99, 134

McKhann G, Drachman D, Folstein, M., et al., Clinical diagnosis of Alzheimer's disease: report of the NINDS-ADRDA work group under the auspices of Department of Health and Human Services Task Force on Alzheimer's Disease. 1984, Neurology 34, 939-944.

Mormann F, Lehnertz K, David P, Elger CE (2000) Mean phase coherence as a measure for phase synchronization and its application to the EEG of epilepsy patients. Physica D. 144: 358-369.

Mormann F, Kreuz T, Andrzejak RG, David P, Lehnertz K, Elger CE (2003) Epileptic seizures are preceded by a decrease in synchronization. Epilepsy Res. 53(3): 173-185.

Novak V, Reeves L, Novak P, Low A, Sharbrough W. (1999). Time-frequency mapping of R-R interval during complex partial seizures of temporal lobe origin. J Auton Nerv Syst 77: 195-202.

Nunez PL, Srinivasan R., Westdorp AF, et al., EEG coherency I: statistics, reference electrode, volume conduction, Laplacians, cortical imaging, and interpretation at multiple scales. Electroencephalogr Clin Neurophysiol. 1997; 103, 499– 515.

Otnes R, Enochson L. (1972) Digital Time Series Analysis, John Wiley & Sons, New York.

Ott E. Chaos in dynamical systems. Cambridge, UK: Cambridge University Press, 1993.

Prichard D, Theiler J (1994) Generating surrogate data for time series with several simultaneously measured variables. Phys. Rev. Lett. 73: 951–954.

Ponten SC, Bartolomei F, Stam CJ (2007) Small-world Networks and Epilepsy: Graph Theoretical Analysis of Intracerebrally Recorded Mesial Temporal Lobe Seizures. Clinical Neurophysiology. 118: 918 – 927.

Rajna P, Clemens B, Csibri E, et al., (1997) Hungarian multicentre epidemiologic study of the warning and initial symptoms (prodrome, aura) of epileptic seizures. Seizure; 6: 361-68.

Rosen I. Electroencephalography as a diagnostic tool in dementia; a review. Acta Neurol Scand Suppl. 1996; 168: 63–70.

Rosenblum M, Pikovsky A, Kurths J, Schafer C, and Tass P. (2001) Phase synchronization: from theory to data analysis, Handbook of Biological Physics,

Elsevier Science, Series Editor A.J. Ho, Vol. 4, Neuro-informatics, Editors: F. Moss and S. Gielen, Chapter 9, pp. 279-321.

Savit R, Green M (1991) Time Series and Dependent Variables. Physica D. 50, 95.

Schack B, Vath N, Petsche H, et al., Phase-coupling of theta-gamma EEG rhythms during short-term memory processing. International J Psychophysiol. 44(2);2002:143-63.

Schindler K, Wiest R., Kollar M, and Donati F. (2002) "EEG analysis with simulated neuronal cell models helps to detect pre-seizure changes", Clin. Neurophysiol. 113, 604–614.

Schreiber T, Schmitz A (2000) Surrogate time series. Physics D 142: 346–382.

Schuster HG. Deterministic chaos. 2nd ed. Weinheim: VCH–Verlag, 1989.

Seeley W, Matthews B, Crawford R, Gorno-Tempini M, Foti D, Mackenzie I, Miller B. 2008. Unravelling Bolero: progressive alphsia, transmodal creativity and the right posterior neocortex. Brain 131, 39-49.

Stam CJ, Jelles B, Achtereekte HA, Rombouts SA, Slaets JP, Keunen RW. 1995. Investigation of EEG non-linearity in dementia and Parkinson's disease. Electroencephalogr Clin Neurophysiol 95:309–317.

Stam CJ, Jones BF, Manshanden I, et al., Magnetoencephalographic evaluation of resting-state functional connectivity in Alzheimer's disease. NeuroImage 2006; 32, 1335–134.

Tass P, Rosenblum MG, Weule J, Kurths J, Pikovsky A, Volkmann J, Schnitzler A, and Freund HJ. (1998) "Detection of n:m Phase Locking from Noisy Data: Application to Magnetoencephalography", Phys. Rev. Lett. 81, 3291

Thompson PM, Moussai J, Zohoori S, et al., Cortical variability and asymmetry in normal aging and Alzheimer's disease. Cerebral Cortex 1998; 8; 492-509.

Valachovic AM, Smith B, Elisevich K, Jacobson G, Fisk J. 1998. Language and its management in the surgical epilepsy patient, in: Johnson, A.F., Jacobson, B.H. (Eds.), Medical Speech–Language Pathology. Thieme, New York, pp. 425–466.

Van der Hiele K, Vein AA, Kramer CG, et al., Memory activation enhances EEG abnormality in mild cognitive impairment. Neurobiol Aging, 2006 ([electronic publication ahead of print] PMID: 16406153).

Weinand M, Carter L, el-Saadany W, Sioutos P, Labiner D, Oommen K. (1997). Cerebral blood ow and temporal lobe epileptogenicity. J Neurosurg 1997; 86:
226-32.

Wu K, Brock W, Savit R (1993) Statistical Tests for Deterministic Effects in Complex Time Series. Physica D. 69, 172.

Xu J, Liu ZR, Liu R, Yang QF. Information transmission in human cerebral cortex. Physica D 1997;106:363-374.

Yates R and Goodman D, 2005. Probability and Stochastic Processes: A Friendly Introduction for Electrical and Computer Engineers. John Wiley & Sons.

Zhang J, Li D, and Savit R. (2009a) “Interictal and Preictal Phase Coherence from Scalp EEG in Focal Epilepsy” (submitted to Epilepsia)

Zhang J, Hudson L, Minecan D, and Savit R. (2009b) Spatial Distribution of Preictal Changes in Phase Coherence from Scalp EEG in Temporal Lobe Epilepsy, submitted to J. Clin. Neurophys.